Imperial College London

On the Benincasa-Dowker Conjecture

Filippo Bounous

Supervised by Professor Fay Dowker

Imperial College London
Faculty of Natural Sciences
Department of Physics
Theoretical Physics Group

Submitted in partial fulfilment of the requirements for the degree of Master of Science, Quantum Fields and Fundamental Forces

September 2022

Abstract

The Causal Set programme is an approach to quantum gravity. It maintains that nature is fundamentally discrete and that all spacetime events are related (or not) through causality. This work provides a brief review of this approach: starting by showing how these two axioms fully define the geometry, moving to the kinematic construction of a causal set; and how it develops dynamically; to the origin of the family of Benincasa-Dowker-Glaser actions. The final aim of this project is to study the behaviour of such an action in the continuum. Benincasa and Dowker postulate that in the continuum limit, the mean discrete action tends to the expected Einstein-Hilbert term plus boundary terms due to the geometry of the spacetime. This conjecture is successfully verified for a four-dimensional slab embedded in flat Minkowski spacetime. A second interest of this thesis is to confirm an unjustified assumption regarding the boundary of support of a scalar field made by Belenchia et al. when investigating the continuum limit of the four-dimensional causal set scalar d'Alembertian.

Ai miei nonni e nonni-zii

"As for me, I am tormented with an everlasting itch for things remote. I love to sail forbidden seas, and land on barbarous coasts."

Herman Melville in *Moby-Dick; or, The Whale*

Acknowledgements

First and foremost, I want to thank Professor Fay Dowker for being all I could ask for in a supervisor. This work would have never been possible without her constant guidance, ceaseless patience, and incredible wisdom: she inspired me every step of the way. I would also like to thank (in alphabetical order): Anantya, Cameron and Raymond for their suggestions; Emma for the discussions and support; and Lorenzo for his advice and comments. Finally, I would like to thank all those countless others who have been by my side along the way. None of this would have been possible without each of you.

F.

Contents

List of Figures

Chapter 1

Introduction

1.1 Quantum Gravity

Since the development of Quantum Mechanics and the theory of General Relativity, numerous attempts have been made toward developing a theory of Quantum Gravity, that is, a framework within which gravity can be described quantum mechanically. It is often described as a major constituent of a grander Theory of Everything. Still, although it would be elegant and satisfactory to have, there is no a priori apparent reason for why this should be the case.

Ever since these two theories were proposed in the early 20th century, they have revolutionised the understanding of the universe and, in many ways, given new perspectives. The former describes the quantum world and interactions between the many elementary particles of which the universe is made up. On the other hand, the latter explains physics on the largest of scales: from planet formation and galaxy mechanics to the evolution of the universe itself. The impact of these two theories cannot be understated: together with Thermodynamics, they have acted as the bedrock to most, if not all, of current physics. Although so much has been built up in some shape or form from these theories, each has shortcomings.

While quantum mechanics is the current best theory for particle physics and goes

a long way in explaining the intricacies of the Standard Model, it fails to provide a good theory for gravity. Similarly, general relativity is the current best theory for gravity. Still, one can find problems built within it: amongst others, singularities appear when analysed at small scales, such as at the Big Bang or inside black holes. Nevertheless, Einstein's field equations,

$$G_{\mu\nu} = 8\pi T_{\mu\nu} \,, \tag{1.1}$$

couple spacetime, an idea from general relativity through the Einstein tensor $G_{\mu\nu}$, to matter, described quantum mechanically through the energy-momentum tensor $T_{\mu\nu}$. This equality suggests some link between the two theories may exist, providing a clear motivation for the study of a theory for quantum gravity.

Several difficulties arise when trying to unify the two. The former's framework is discrete and probabilistic: asking a question does not result in a binary answer; it results in an amplitude from which the probability of a given process happening may be calculated. The latter is continuous and deterministic: events are just points connected by worldlines. These differences make it remarkably difficult to create a correspondence between the two, as the same questions cannot always be posed when questioning reality. Nevertheless, plenty have tried.

The many approaches proposed differ significantly: when looking at loop quantum gravity [4] compared to string theory [5], this becomes most apparent. A lack of coherence and agreement on the fundamental principles may be traced to a deficit in experimental support. Contrary to the past, where experiments hinted at the direction to take and so somewhat guided the theory, research is near blind this time around. The study of quantum gravity remains heavily theoretical with a plethora of approaches.

Despite this lack of suggestions, another major problem in the current understanding of physics gives an even bigger reason to look for a unified theory: infinities

appear. Should the origin of these singularities not be physical objects but mathematical artefacts, it suggests the theories are incomplete.

1.2 Problems Arising in the Continuum

The fact that general relativity is built upon a continuous Lorentzian manifold does not necessarily mean that a continuous manifold must be fundamental. Nevertheless, one may want to find more reasons to disregard it as a fundamental aspect of the theory. In the present understanding of physics, three infinities appear: quantum mechanics and general relativity have one each, while the third is due to quantum gravity proper [6].

In quantum mechanics, or better in what is used to deal with it relativistically, Quantum Field Theory, infinities appear when length scales are taken to be arbitrarily small (i.e. energy scales to be arbitrarily large), this is symbolised by $Z = \infty$. For a renormalisable theory, the problem is solved through renormalisation, that is, by redefining the Lagrangian using a finite number of counter-terms to absorb all these divergent terms [7]. However, gravity appears to be non-renormalisable as all the divergences cannot be absorbed using a finite number of counter-terms [8, 9, 10]. This issue could be solved by imposing a *physical* cutoff limit on the energy scale, essentially fixing a lower bound for distances.

In general relativity, the infinities are evident, and $R_{\alpha\beta\gamma\delta} = \infty$ symbolises them. There exist regions of infinite curvature, such as those inside a black hole's event horizon, in what, if not, would be a perfectly regular spacetime manifold. When the radius around these singularities is taken to be on arbitrarily small scales is when these infinities are faced [11]. There are compelling arguments for these objects to exist after the successful detection of gravitational waves by LIGO-Virgo in 2015, followed by infrared detection in 2019 [12, 13]. However, the infinite tidal forces that general relativity predicts are believed to be unphysical. These tidal forces

are thought to a manifestation of the breaking down of the theory at the quantum scale, in the immediate vicinity of the singularity, justified by the fact that general relativity is not a quantum theory. For similar reasons, it fails in the very early universe.

Last but not least, the final infinity appears in quantum gravity, symbolised by $S_{BH} = \infty$. It is the infinite entropy of the black hole, appearing when counting the number of degrees of freedom of the event horizon [14]. However, Stephen Hawking's black hole entropy formula gives a finite answer, suggesting the complete picture is yet to be found [11, 15].

The origin and character of these infinities give some hints as to what a theory of quantum gravity should look like: it should be able to recover both quantum field theory and general relativity in the classical limits and round them off by describing the smallest-scale physics. There also are further suggestions as to why a Theory of Everything may be lurking out there: the different interpretations of reality of the two theories indicate something is missing, and the fact they both break down in specific regimes suggests they are not the fundamental answer. Most importantly for Causal Set Theory, the nature of these divergences infers that there might be a minimum length scale, a discreteness scale, built into nature beyond which physics is no longer applicable. This construction directly contradicts general relativity and quantum field theory, but may it be the answer we have long been looking for?

Chapter 2

Causal Set Theory

In addition to the difficulties described earlier, on the path to constructing a theory for quantum gravity, many crossroads are reached and one must pick a direction each time. Some of these questions, as described by Rafael Sorkin [16], include: (a) the sum-over-histories framework or the "observable and state-vector" approach; (b) relative probabilities or absolute ones; and (c) a differentiable manifold or a discrete underlying structure?

With these forks in mind and the conclusions drawn from the divergences, a theory with discreteness at its very core was developed.

2.1 Origins

The idea that space may be discrete is not novel: it can be traced back to Riemann in recent times and even further to Zeno. The former, in his inaugural lecture that laid down the foundations of geometry and curvature, said [17]:

> "The question of the validity of the presuppositions of geometry in the infinitely small hangs together with the question of the inner ground of the metric relationships of space. In connection with the latter question... the above remark applies, that for a discrete manifold, the principle of its

> metric relationships is already contained in the concept of the manifold itself, whereas for a continuous manifold, it must come from somewhere else. Therefore, either the reality which underlies physical space must form a discrete manifold or else the basis of its metric relationships should be sought for outside it."

Here Riemann essentially wonders what exactly it is about continuous space that allows us to discuss measurable things such as lengths, areas, etc. He contrasts the origin of these in a discrete manifold, where they are inherently built in, to a continuous manifold where the metric structure must be sourced from elsewhere. Over a century later, Einstein, after having already adopted Riemann's notion of a continuum in general relativity, doubted whether this idea could persist [18]:

> "In any case, it seems to me that the alternative continuum-discontinuum is a genuine alternative; i.e. there is no compromise here. In [a discontinuum] theory there cannot be space and time, only numbers. It will be especially difficult to elicit something like a spatio-temporal quasi-order from such a schema. I can not picture to myself how the axiomatic framework of such a physics could look. But I hold it as altogether possible that developments will lead there."

Einstein shines a light on the importance of causal order and how difficult it would be to derive it purely from an algebraic scheme. However, causal set theory precisely incorporates this ordering by construction: it and discreteness are the inherent components of the theory.

Order + Number = Geometry

We may now appreciate how the full geometry of spacetime can be recovered from these two notions alone. According to general relativity, each four-dimensional spacetime point can be fully defined using ten numbers due to the ten independent components of the Einstein tensor, $G_{\mu\nu}$.

Nine of these numbers may be found just from knowing how light propagates through spacetime. Let us consider the lightcone and notice how it can be defined in causal terms [19]. Taking the event at the origin as a reference point, it can be said that those events on or inside the future cone are influenced by the starting element, while it is influenced by those in its past light cone. These spacetime events are said to be *causally related* to the reference event. Then, all those outside the cone are said to be *causally unrelated* to the original point. Simply using this idea of causality, a *causal order* (or lack thereof in the latter case) has been defined. Similarly, one can work backwards: from the causal order of spacetime events, the light cones of spacetime events can be recovered, and from these, it is possible to retrieve nine of the ten numbers.

Formally, a theorem by Hawking, King, McCarthy [20] and Malament [21], referred to as the "HKMM" theorem by Surya [22]:

Theorem 1 (HKMM)**.** *If there exists a chronological bijection f_b between two d-dimensional spacetimes which are both future and past distinguishing, then these spacetimes are conformally isometric when $d > 2$.*

Where the future and past distinguishing spacetimes are those in which, for all events p in the spacetime, its chronological past and future $J^{\pm}(p)$ is unique. Thus, if $J^{\pm}(p) = J^{\pm}(p) \implies p = q$. Levichev subsequently showed that this statement is equivalent for *causal* instead of *chronological* ordering [23]. These two results highlight how if two spacetimes possess identical causal structure, they are conformally isometric.

The metric has then been recovered up to a conformal rescaling factor, so the missing piece of information is given by encoding the volume of spacetime. In the context of *discrete* order, the number of discrete elements can be equated to the volume simply by counting them as there will be finitely many. One may appreciate how this notion of discreteness follows naturally from a theory with causality at heart; all this can be done without relying on any extra outside information. In the

context of a continuous manifold, counting would have resulted in an uncountably infinite large number of elements [19]. Thus leading to the need for an externally-sourced volume element of the form, $dV = \sqrt{-g}\, d^4x$.

Clearly, the geometry of spacetime has now been fully defined, having found all ten numbers. R. Sorkin's famous slogan encapsulates this idea:

$$Order + Number = Geometry\,. \tag{2.1}$$

The Discreteness Scale

When discussing a discrete theory, it is imperative to address the scale at which this discreteness takes place. One established approach in defining this is through the black hole horizon entropy [19], some careful considerations lead the length scale to be defined as:

$$l_P = \sqrt{\frac{8\pi G\hbar}{c^3}}\,, \tag{2.2}$$

which is precisely the Planck length. The size of these elements suggests why we have not experienced the granularity of spacetime; it is just too small for current technology to detect. Assuming that each fundamental volume, $V \sim l^4$, contains exactly one spacetime event, then one cubic centimetre for one second would contain $\sim 10^{139}$ elements, an enormous number. It should also be noted that in the classical limit ($\hbar \to 0$), $l \to 0$ and so the recovery of the continuum as expected.

Phenomenology

Causal set theory has also had an important phenomenological success. Recent considerable advances in astronomical observations have shed light on the value of the cosmological constant Λ. The seemingly correct agreement between the experimental measurement and the theoretical prediction of the order of magnitude of Λ [19], has obviously been an enormous success for causal sets.

In this theory, the discrete manifolds are made up from a random Poisson pro-

cess known as "sprinkling", described in section 2.5. This random process implies that Λ must fluctuate around its target, expected, value. The magnitude of these fluctuations decreases in time like $\sqrt{N}$ where N is the relevant number of *ancestors* (see section 2.2) of a causal set element at a given cosmological epoch [19]. The target value has been suggested to be zero, with these fluctuations just being an artefact of the statistical process. This leads to the proposed relation [24]:

$$\Lambda \sim \frac{1}{\sqrt{N}} \,. \tag{2.3}$$

For the observable universe (to date) $N \sim 10^{240}$, and so $\Lambda \sim 10^{-120}$ which is in agreement with observations [19]. This prediction, however, still remains purely heuristic until a complete Quantum Causal Set Dynamics (see section 2.8) is formulated.

2.2 Definitions

Let us start with the most important definition to our project.

Definition 2.1. A causal set (or *causet* for short) is defined to be a locally finite partial order (*poset*) whose order is governed by causal order. Formally, it is a pair $(\mathcal{C}, \preceq)$ made up of a set, $\mathcal{C}$, together with a partial order relation, $\preceq$, with the following properties:

1. **Reflexivity**: $\forall x \in \mathcal{C},\ x \preceq x$;

2. **Transitivity**: $\forall x, y, z \in \mathcal{C},\ x \preceq y \preceq z \implies x \preceq z$;

3. **Acylicity**: $\forall x, y \in \mathcal{C},\ x \preceq y \preceq x \implies x = y$;

4. **Local finiteness**: $\forall x, y \in \mathcal{C},\ |I(x,y)| < \infty$, where we have that the set $I(x,y) := \{z \in \mathcal{C} \mid x \preceq z \preceq y\}$ is an order interval and $|S|$ is the cardinality of a set S.

We will say that, given $x \preceq y$, then x *precedes* y.

The above four properties give the complete structure of the causet. *Reflexivity* is the most intuitive; it means that all elements of the causet precede or are equal to themselves. *Transitivity* means that if X and Y are causally related, and Y is also causally related to Z. Then, there exists a causal relation between X and Z (even just by moving through Y). *Acylicity* means there can be no closed loops. This can be seen by considering a causal set $\{x, y, z, w \in \mathcal{C} \mid x \prec y \prec z \prec x,\, x \prec w\}$ that is, a loop of x, y, z connected to a final element w through x. From the point of view of w, by transitivity, each of the three elements in the loop precedes it, becoming indistinguishable. This indistinguishability does not allow one to define notions such as distance, and so it becomes impossible to build up a Lorentzian manifold from the causet. Finally, *local finiteness* is the condition through which spacetime discreteness enters the picture. In a continuous spacetime, any causal interval will contain an uncountably infinite number of events, and so by not allowing this, notion of discreteness has been introduced.

Several other notions are also to be introduced, these will become useful in later sections and chapters:

- If $x \preceq y$ but $x \neq y$, we say $x \prec y$ where $\prec$ is known as a *strict causal relation* given by an irreflexive relation.
- If $x \not\preceq y$ and $y \not\preceq x$, the elements are *unrelated*, we say $x||y$.
- If $x \prec y$ then x is an *ancestor* of y, likewise y is a *descendant* of x.
- If $x \prec y$ and $n(x, y) := |I(x, y)| - 2 = 0$, we say there is a *link* between the two elements. Links are the irreducible elements of a causet; we say $x \prec *y$.
- Given an element $x \in \mathcal{C}$, we define the set of all its past nearest neighbours as the first *past layer*. In general the i-th past layer is given by the set of $y \in \mathcal{C}$ such that $y \prec x$ and $n(x, y) = i - 1$. Similarly, this may be repeated for the *future layers*.

- If $\forall x, y \in \mathcal{C}' \subset \mathcal{C}$ there exists a relation between them, that is, either $x \preceq y$ or $y \preceq x$, then $\mathcal{C}'$ is a linearly ordered subset, a *chain*.

- If $\forall x, y \in \mathcal{C}' \subset \mathcal{C}$ there does not exist a relation, that is, $x||y$, then $\mathcal{C}'$ is a totally unordered subset, an *antichain*.

- A chain is a *path* if all the relations between adjacent elements are a link.

- A path between x, y is *maximal* if it has maximal cardinality between all possible paths, and respectively for *minimal*. These maximal chains are the causet analogue of timelike geodesics in the continuum.

2.3 Representations

Causets can be represented by "Hasse" diagrams, originally used to visualise posets. Hasse diagrams ignore all connections which are not links, $\prec *$, the transitivity property can be used to deduce all other relations. If we have $x \prec *y$ then we draw x below y such that causal order flows upwards, with a line in between to represent the link, as seen on Fig. 2.1(a). This in contrast to directed graphs in which *all* relations are explicitly shown, see Fig. 2.1(b). Let us consider an example, for a causet $(\mathcal{C}, \preceq)$ with the following relations:

$$\begin{gathered} \mathcal{C} = \{x, y, z, w\}\,, \\ x \preceq x\,, \quad x \preceq z\,, \quad x \preceq w\,, \\ y \preceq y\,, \quad y \preceq z\,, \quad y \preceq w\,, \\ z \preceq z\,, \quad z \preceq w\,, \\ w \preceq w\,, \end{gathered} \tag{2.4}$$

which satisfies the four axioms of causets. It is shown diagrammatically in Fig 2.1.

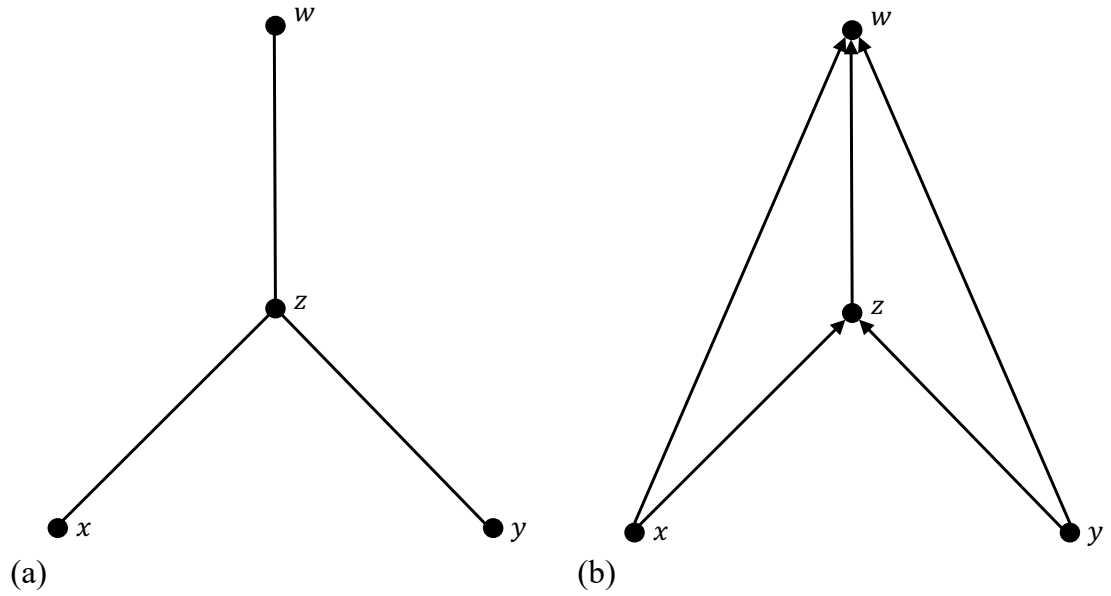

Figure 2.1: Hasse and directed graphs as representations for a causal set $\mathcal{C}$. (a) A Hasse diagram for the causal set, only links are shown. (b) The directed graph of the causal set, with all relations explicitly shown and where arrows represent causal order.

2.4 Embeddings

A major issue with introducing discreteness is that it must be possible to recover the continuum from it, as required by the prior considerations regarding what a theory of quantum gravity should look like. We must then ask ourselves what we require to claim that a spacetime $(\mathcal{M}, g)$ is an appropriate approximation of the underlying causet $(\mathcal{C}, \preceq)$. First of all, the notion of a *faithful* embedding is needed [22]:

Definition 2.2. An *embedding* of a causet $(\mathcal{C}, \preceq)$ into a Lorentzian manifold $(\mathcal{M}, g)$ is a map:

$$f : \mathcal{C} \to \mathcal{M}\,, \tag{2.5}$$

such that the causal structure is preserved, that is, for causally related elements:

$$x \preceq y \in \mathcal{C} \Longleftrightarrow f(x) \preceq f(y) \in \mathcal{M}\,, \tag{2.6}$$

i.e. there exists a future directed causal curve connecting them. Similarly, if there

is no relation between two elements, they will be spacelike separated.

Definition 2.3. A *faithful embedding* is an embedding for which there is a map:

$$f : \mathcal{C} \to \mathcal{M}\,, \tag{2.7}$$

such that $f(\mathcal{C})$ is uniformly distributed in $(\mathcal{M}, g)$ at density ρ, with respect to the volume measure on $\mathcal{M}$.

The thinking is then restricted to scales over which the variation of the geometry on the manifold is much larger than the embedding scale. With this, there is the *Hauptvermutung*, or fundamental conjecture, of causal set theory [19]:

Conjecture 2.1 (Hauptvermutung)**.** *If a causet $(\mathcal{C}, \preceq)$ can be faithfully embedded with density ρ into two distinct Lorentzian manifolds $(\mathcal{M}, g)$, $(\mathcal{M}', g')$ then the two manifolds are "approximately isometric".*

What is very important to notice is the use of the word "approximately"; this is as on scales smaller than the discreteness scale, there no longer is a faithful embedding, consequently the two manifolds may differ at the Planckian scale.

2.5 Sprinklings

Having discussed the faithful embedding of a causet into a manifold, it must be possible to reverse the process. Having also reached the realisation that not all causets may be easily embedded into Lorentzian manifolds, the thinking is restricted to those which can. This is done by reversing the method, that is, producing a causet from a causal Lorentzian manifold, achieved through a random process known as *sprinkling*.

When deciding what random process to turn to, the manifold's properties and the causet's requirements must be considered. The spacetime is known to possess

Lorentz invariance by construction, and this property must persist. That is, the causet should not choose a particular direction in spacetime.

Should the choice be made to place points in a uniform lattice, they would naively appear to be equally spaced. However, as soon as a Lorentz transform is performed (for instance, a boost), the spacing will lose its uniformity, and statistically, they will differ. This is not a Lorentz invariant choice and as such must be discarded [19].

A second approach is to use a random Poisson distribution to place the points, this does in fact lead to a Lorentz invariant formalism [22].

The Poisson Process

A Poisson process is just a limiting case of a binomial process, B_r [25]. Let us consider a continuous manifold, $\mathcal{M}$, and divide it into n equal cells. Each cell has volume $V_n = \frac{V}{n}$, where $V = \mathrm{vol}\,(\mathcal{M})$. A point is then independently placed in each such cell with probability p_n. The expected number of points in R then is:

$$\langle N \rangle = p_n n = \rho V\,, \tag{2.8}$$

where $\rho = \frac{\langle N \rangle}{V}$ is the density of points.

The limiting case is to be considered $n \to \infty$, i.e. the continuum. For a general number of points $N = k$, the binomial probability of placing k points in n cells of the lattice is given by:

$$P\,(k) = (1 - p_n)^{n-k}\, p_n^k \binom{n}{k}\,, \tag{2.9}$$

after some manipulation; and by using $\mu = \rho V$:

$$P(k) = \frac{n!}{(n-k)!\; n^k} \left(1 - \frac{\mu}{n}\right)^n \frac{\mu}{k!}^k \left(1 - \frac{\mu}{n}\right)^{-k}\,. \tag{2.10}$$

As continuum limit is being considered, the following limits are taken into account:

$$\lim_{n\to\infty} \frac{n!}{(n-k)!\; n^k} = 1\,, \tag{2.11}$$

$$\lim_{n\to\infty} \left(1 - \frac{\mu}{n}\right)^n = e^{-\mu}\,, \tag{2.12}$$

$$\lim_{n\to\infty} \left(1 - \frac{\mu}{n}\right)^{-k} = 1\,. \tag{2.13}$$

Reassembling everything, the continuum limits recovers the promised Poisson distribution:

$$P\,(k) = \frac{(\rho V)^k\, e^{-\rho V}}{k!}\,. \tag{2.14}$$

Precisely, this is the probability of a causet, $\mathcal{C}$, having k points in a volume V with density ρ.

It has been shown that this framework is Lorentz invariant, as required [26]. This is given by the fact that, although points will change position and coordinates under a Lorentz transform, their macroscopic distribution will hold. And so, statistically, they will be indistinguishable. This property holds due to the fact that the Poisson distribution is based upon Lorentz invariant quantities: V is constant regardless of the frame of reference, and so is the expected number of points $\langle N\rangle = \rho V$. This may produce a causet, as seen in Fig. 2.2 for 600 elements sprinkled in a finite causal interval in $(1+1)$-dimensional Minkwoski spacetime.

After sprinkling, the causal relations between points are imposed using the original manifold's causal order, i.e. light cones. It is then said that a causet $\mathcal{C}$ is well-approximated by a spacetime $(\mathcal{M}, g)$ if it could have been generated with relatively high probability by a sprinkling process. It should be noted how this is a *kinematical* process of producing a causet, dynamically the story will be different; see Sec. 2.8.

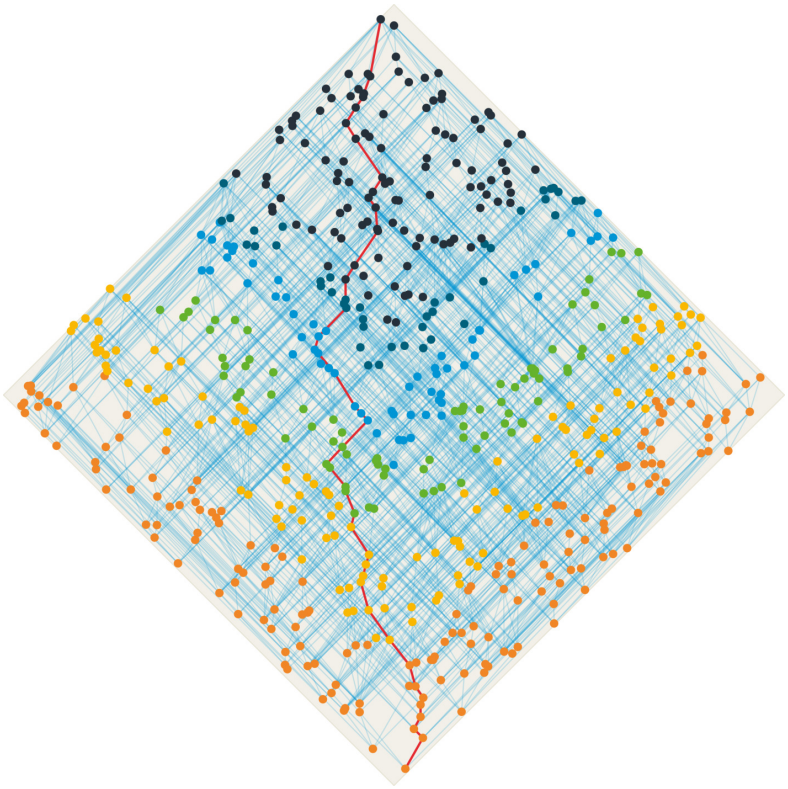

Figure 2.2: A sprinkling of 600 elements into a finite interval in $(1+1)$-dimensional Minkowski spacetime [1], having imposed causal relations. The red line connecting the past-most and future-most events shows a possible maximal path.

2.6 Coarse-Grainings

A further aspect that may investigated in the approach to finding a link between discreteness and the continuum is *coarse-graining*. For a spacetime $(\mathcal{M}, g)$ it is possible to obtain a causet $(\mathcal{C}, \preceq)$ for different densities, ρ. Given a causet $(\mathcal{C}, \preceq)$, which may or may not faithfully embed into a spacetime $(\mathcal{M}, g)$, we may *coarse-grain* it into a smaller subcauset $\mathcal{C}' \subset \mathcal{C}$ which faithfully embeds into $(\mathcal{M}, g)$ at $\rho' < \rho$ [19, 22]. Coarse-graining can be thought of as an "averaging" over the original elements. For example, let us consider a random selection of elements in $\mathcal{C}$ such that for every n elements in $\mathcal{C}$, $n' = (\rho'/\rho)\, n$ are chosen [22], is a coarse-graining. A second example may be made to the sprinkling process itself applied to the causet [19], by assigning a fixed probability p_x of keeping each element $x \in \mathcal{C}$.

Then, for instance, for a $3:1$ coarse-graining we may choose $p_x = 1/3$.

This broader condition can be considered an "intermediate" stage of the embedding process. It allows us to take in more causets that are not manifold-like at the Planck scale, but could still have physical manifestations. This allows the consideration and study of a wider range of causets, for instance, those of microscopic states in the quantum regime. Through coarse-graining, it is possible to define a subcauset which in turn can be faithfully embedded into a continuous spacetime.

2.7 Dimensions

Before tackling the dynamics of causal set theory, one should investigate a final aspect of the manifold approximation: its geometry and topology. Assuming the Hauptvermutung is true, it is possible to extract geometrical and topological information from the manifold's order relation. A most fundamental aspect of the manifold's topology, of interest to us, is its dimension. Dimensionality is not an inherent property of a causet, so it is possible to arrive at the effective continuum dimension of the causet in various ways; three will be presented [19]. All three estimators determine a dimension for an interval I in a causet $\mathcal{C}$ for the case where $I \approx A$. Here A is a double light cone interval (also known as an Alexandrov interval or, colloquially, a causal diamond), in Minkowski space $\mathbb{M}^d$.

Myrheim-Meyer Dimension

Given an order interval $I(x, y)$ for $x, y \in \mathcal{C}$ where $x \preceq y$, then let $N(x, y) = |I(x, y)|$ be the number of elements within the order interval and R be the number of relations, that is, pairs $x, y \in I(x, y)$ such that $x \preceq y$. Also, let:

$$f(d) = \frac{3}{2}\binom{3d/2}{d}^{-1}. \tag{2.15}$$

Finally, an estimate for the dimension when $N \gg \left(\frac{2}{7}/16\right)^d$ is given by [27, 28]:

$$d = f^{-1}\frac{R}{\binom{N}{2}} = f^{-1}\frac{R}{N\left(N-1\right)}\,, \tag{2.16}$$

which means an estimate of the dimensions of the causet can be found by counting the number of elements and the number of relations between them. Then, for a fixed number of elements, a higher number of relations will lead to a higher dimensionality.

Midpoint Scaling Dimension

Given an order interval $I\left(x,y\right)$ for $x,y \in \mathcal{C}$ where $x \preceq y$, let $z \in I$ such that $x \prec z \prec y$. Next, let us define two new order intervals $I_1\left(x,z\right)$ and $I_2\left(z,y\right)$ for which $N_1\left(x,z\right) = \left|I_1\left(x,z\right)\right|$ and $N_2\left(z,y\right) = \left|I_2\left(z,y\right)\right|$.

We choose z to be the "midpoint", that is, to maximise

$$N_{mid} = \min\{N_1\left(x,z\right), N_2\left(z,y\right)\}\,. \tag{2.17}$$

The dimension of the causet $\mathcal{C}$ is then defined as [29, 30]:

$$d = \log_2\left(\frac{N}{N_{mid}}\right)\,. \tag{2.18}$$

A Third Estimator

Given an order interval $I\left(x,y\right)$ for $x,y \in \mathcal{C}$ where $x \preceq y$, then let $N\left(x,y\right) = \left|I\left(x,y\right)\right|$ be the number of elements within the order interval and K be the number of chains in $I\left(x,y\right)$. Then, another estimation of the dimensionality is given by [19]:

$$d = \frac{\ln N}{\ln\ln K}\,. \tag{2.19}$$

However, it should be noted that this is only a reasonable estimate for exponentially large N due to the logarithmic relation.

2.8 Dynamics

So far, all we have is what a causal set is and how a spacetime can be associated to it; we are yet to produce the laws of motion; we have *kinematics without dynamics*. To formulate a theory of Quantum Gravity, these dynamics are expected to be quantum in character, but we cannot start directly from a quantum dynamics. Let us begin from the idea that a causet develops in time, or better, that the growth of a causet is time *itself*, in a process known as "sequential growth". As we would like a quantum dynamics, this process will be of probabilistic nature (classically at first and quantum at a later stage). Essentially the aim is to develop a quantum dynamics starting from a classical stochastic process [19].

Classical Sequential Growth

This first stochastic process is known as a "Classical Sequential Growth" model (CSG) and was introduced by Rideout and Sorkin [31]. The dynamics is described as a series of "births" of new causet elements with assigned probability to each possible path. However, clearly, this is much too loose, and the sheer number of choices gets us nowhere, especially seeing how many would result in completely unphysical causets. As a result, some physical restrictions are imposed on the process [19].

First of all, we impose *internal temporality*, this ensures causality is respected. We prohibit an element being born "before" one which causally precedes it. Elements can only be born in the causal future of, or spacelike to, all already existing elements. This introduces a natural labelling of non-negative integers purely based off of "fictitious" birth order, such that:

$$x \prec y \implies \text{label}\,(x) < \text{label}\,(y)\,. \tag{2.20}$$

For example, the first-born is "0", the second-born "1" and so forth. However, this can be seen as a gauge choice.

Secondly, there is the introduction of *discrete general covariance*. This statement is very similar to one present in general relativity. We want our framework to be independent of its natural labelling, precisely to how general relativity is coordinate independent. Should this labelling persist, it would suggest that the elements are governed by some sort of unphysical "external time". Thus, this condition is just a statement about gauge invariance.

Next, there is the necessity of the *Markov sum rule*, that is, all the probabilities of all the possible transitions at any given stage sum to one.

Finally, there is the requirement of *Bell causality*. Loosely, it ensures that the birth of an element in one region of a causet is independent of the births taking place in another region of the causet spacelike to the first.

The resulting family of equations from these conditions may be solved explicitly and in general [31, 32]. At stage n, the transition probability for $c_n^i \rightarrow c_{n+1}^{j(i)}$, $\mathcal{C}^i \rightarrow \mathcal{C}^{j(i)}$ where an element is born with ϖ ancestors and m parents (direct ancestors) is given by:

$$P\left(c_n^i \rightarrow c_{n+1}^{j(i)}\right) = \frac{\lambda\left(\varpi, m\right)}{\lambda\left(n, 0\right)}\,, \tag{2.21}$$

where n is also the cardinality of the original causet $\mathcal{C}^i$ and λ is defined as:

$$\lambda\left(\varpi, m\right) = \sum_{k=m}^{\varpi} \binom{\varpi - m}{k - m} t_k\,, \tag{2.22}$$

with $t_n \geq 0$ and $t_0 > 0$ being viewed as the coupling constants of this dynamics. The result is an infinite number of causets (each of which may be an infinitely long sequence). However, very many of these are of no interest as they do not describe physical spacetimes, while others describe causal set interpretations of known physical notions. Yet, some are interesting and will define physical laws based on the ratios of these constants [19].

This structure, and the growth of causets, can be seen in a partial order of causets, known as a *poscau* diagram. A poscau can be thought of as a *Hasse diagram*

of Hasse diagrams, it represents all the possible dynamic evolutions a given causet can take. Thus, a path through a poscau then corresponds to a sequence of causet transitions given by their respective probabilities. It should be noted that, different paths through a poscau can lead to the same causet. However, by discrete general covariance, this is just an equivalent way of representing the same growth process, and thus the probabilities of reaching either causet are equal. In Fig. 2.3, Henson has made the starting element the empty set, but obviously, one may start from any causet and apply the same rules to see the growth.

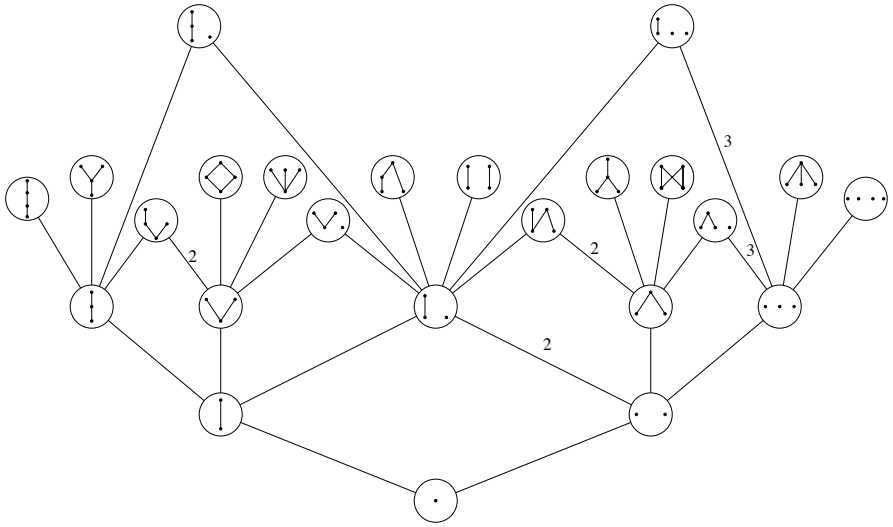

Figure 2.3: A poscau diagram starting from a single element and growing up to causets of cardinality four [2]. Numbered links refer to the different ways the same causet could be generated due to automorphisms of the parent causet. It is important to note that, on the grounds of discrete general covariance, although certain identical causets have different growth paths, they are just equivalent ways of representing the same process and so have the same probabilities of happening.

Quantum Sequential Growth

To move to a quantum sequential growth model (QSG) from a classical one, it must be "quantised". This is done through the use of measure theory: by replacing the classical measure μ_C with a *quantum measure*, μ [33, 34, 35]. We will not go into the details of measure theory; only a very brief introduction to the ideas is provided as the specific details are beyond the scope of this work. Essentially, ther is a classical

measure μ_C (also known as a level 1 measure) which can be related with the classical probabilities of CSG and as such satisfies the Kolmogorov rules (additivity):

$$\mu\left(\alpha \cup \beta\right) = \mu\left(\alpha\right) + \mu\left(\beta\right) \,, \tag{2.23}$$

where α and β are subsets of the set of all possible configurations of past finite causets.

On the other hand, the quantum measure μ (also known as a level 2 measure) cannot be thought of as a "probability" in the classical way as it is allowed to violate the Kolmogorov rules, but respects the quantum sum rule [22]:

$$\mu\left(\alpha \cup \beta \cup \gamma\right) = \mu\left(\alpha \cup \beta\right) + \mu\left(\alpha \cup \beta\right) + \mu\left(\beta \cup \gamma\right) - \mu\left(\alpha\right) - \mu\left(\beta\right) - \mu\left(\gamma\right) \,, \tag{2.24}$$

where α, β, γ again are subsets of all possible past finite causets.

With this new interpretation in mind, to be able to better define a quantum analogue, the classical rules must be re-expressed into quantum language and ensured that μ respects them [35]. The first condition of internal temporality can be implemented identically. To introduce the condition of discrete general covariance, we should first restate the classical requirement using measure theory nomenclature. We say that the measure μ_C must be the same for order isomorphic causets. The quantum equivalent then follows as it requires:

$$|c_n^i\rangle = |c_n^j\rangle \,, \tag{2.25}$$

when $c_n^i \sim c_n^j$. To find the analogue of the Markov sum rule, the quantum counterpart of total probability summing to unity through operators is needed. Specifically for this case, a set of transition operators given by $\widehat{O}\left(c_n^i \to c_{n+1}^{j(i)}\right)$ such that:

$$|c_{n+1}^{j(i)}\rangle = \widehat{O}\left(c_n^i \to c_{n+1}^{j(i)}\right)|c_n^i\rangle \,, \tag{2.26}$$

which must satisfy:

$$\sum_{j(i)} \widehat{O}\left(c_n^i \to c_{n+1}^{j(i)}\right) = \mathbb{I}\,. \tag{2.27}$$

Finally, the Bell causality condition is much more subtle to introduce; this, however, can be done unambiguously when $\mathcal{H} \simeq \mathbb{C}$, as the transition operators simplify to $\mathbb{C}$-valued amplitudes [35].

Although QSG has had a lot of progress in recent years, a lot remains to do and be discovered, it is still in its infancy and a full quantum dynamics requires much work.

A quantum dynamics is built in the hope of reproducing a fully functioning theory of quantum gravity, but at a fundamental level, it looks very different. This theory must be formalised in order to create a stronger parallel, which can be done in various ways. The question that must be asked is whether a sum-over-histories framework or the "observable and state-vector" approach would work best. Or, expressed differently, should a path integral approach to quantum mechanics or the canonical formulation of quantum theory be used.

Given a choice between the use of a Lagrangian or a Hamiltonian to solve this problem, the understanding is to side with the former. The Hamiltonian approach requires the unphysical separation of time from space as it requires an external time parameter with respect to which the system then evolves. This feels completely unnatural to do, seeing as space and time are indistinguishable at the causet level [6, 19]. Monte-Carlo simulations of the action have been performed, and promising evidence has been collected, specifically for the two-dimensional continuum case [36]. Finally, using the Lagrangian approach, one is able to employ a sum over histories (path integral) approach. The causet analogue to the sum over all the possible trajectories a particle could take is the sum over all possible causets that could, in principle, be grown. The discretised version (in the continuum this would be an

integral), takes the form:

$$Z = \sum_{\mathcal{C}} e^{i\mathcal{S}[\mathcal{C}]}\,, \tag{2.28}$$

to be able to define this we now need a *causet action* $\mathcal{S}\,[\mathcal{C}]$.

Chapter 3

The Action of a Causal Set

As mentioned, along the road to quantum gravity, the choice is made to take the sum over histories route to the dynamics, and as a result, a *causet action*, $\mathcal{S}(\mathcal{C})$, is required. To recover the current theories, the causet action is expected to recover the Einstein-Hilbert action (Eq. 3.19) in the continuum limit. Thus, an action will be built up from this assumption.

3.1 The d'Alembertian

We want to be able to construct a differential operator on the discrete spacetime of causal sets analogously to how it must be done on a continuous manifold. Therefore, more than one element is required. These are the "nearest neighbours" of the point in question, the (past or future) *layers* previously defined.

Non-Locality

Up to this point, a framework has been constructed with Lorentz invariance and discreteness. However, their combination results in a radical (but causal) non-locality [37, 38, 39]. This notion of non-locality could turn out to be fatal: if it cannot be tamed, the inherently local theory of general relativity cannot be recovered. To appreciate its origin, consider a causet faithfully embedded in Minkowski

spacetime. Let us take an element, x, and notice how all its nearest neighbours will be one unit of Planck proper time away from x. The locus of all such points forms a hyperboloid that stretches from past infinity up to future infinity; it will have infinite spatial volume. All elements in the vicinity of such a surface will form links with the initial element and thus be considered x's "nearest neighbours". Clearly, there is an infinite number of such points, and even in the presence of Lorentz-symmetry-limiting curvature, the number of nearest neighbours will remain huge as long as the radius of this curvature is greater than the Planck scale [40]. To align with the sprinkling process, this sentiment may be expressed by saying that the probability of x having a limited number of nearest neighbours is vanishingly small. It is then straightforward to see how problems will arise when attempting to define any notion of "discrete locality" [41].

A causet d'Alembertian is crucial to define the dynamics and equations of motion of a real scalar field φ on a background causet. Having assumed vanishing mass, it is expected that in the continuum limit $\Box\varphi = 0$. This radical non-locality must be confined to the Planck scale, where physics has already been seen to possess this property, and as such will not cause problems. This is achieved by finding cancellations between the "non-local" couplings of the field φ, such that the limit theory may be recovered. To start the construction of the d'Alembertian, let us assume that it acts linearly on φ so that the task simply becomes finding a suitable matrix B_{xy} that plays the role of the d'Alembertian, where $x, y \in \mathcal{C}$. The requirement of causality becomes equivalent to $B_{xy} = 0$ whenever $x \prec y$ or $x||y$ [41].

Recovering the d'Alembertian

To construct the d'Alembertian let us first make some observations about B_{xy}. First of all, for a usual sprinkling, there will be an equal distribution of the individual elements between positive and negative values. Secondly, x has a stronger coupling with elements that are a small proper distance away from it; those with a large

proper distance will make a near-zero contribution. The former, however, seems to be the suggestion that unlocks the puzzle: introducing oscillating signs in the discretised causet d'Alembertian operator. Sorkin explains the justification and thought process behind this method in great detail in [41], a brief summary of it will be presented.

Let us consider the case of $\mathbb{M}^1$, just the real line, where $\Box = \frac{\partial^2}{\partial t^2}\varphi$ up to a sign convention. This differential operator may be discretised with spacing Δt as:

$$\frac{\partial^2}{\partial t^2}\varphi\left(t\right) \approx \frac{1}{\Delta t^2}\varphi\left(t-\Delta t\right) - 2\varphi\left(t\right) + \varphi\left(t+\Delta t\right)\,, \tag{3.1}$$

where the causet analogue would be the three-chain $x \prec *y \prec *z$. A discretised causet d'Alembertian will be built up from these principles.

Now consider a causet sprinkled in $\mathbb{M}^2$ where we want $\Box\varphi|_x$ (note $x \in \mathcal{C}$ has been fixed and our spacing $\Delta t \to l_P$, to agree with the fundamental causet scale). To impose causality, the discretised operator is chosen to be solely dependent on those elements which precede it; we introduce the idea of *past layers* in order to distinguish them. The prescription of $\Box\varphi$ consists of a linear sum of a certain number of layers with alternating signs; it is restricted by requiring it to be causal, Lorentz invariant, and analogous to the d'Alembertian on a lattice. The minimum number of layers requires to ensure the uniqueness of coefficients has a curious sequence, for d dimensions:

$$\begin{aligned} \text{Even } d\text{:} \qquad & L_{\max} \geq \frac{d}{2} + 2\,, \\ \text{Odd } d\text{:} \qquad & L_{\max} \geq \frac{d-1}{2} + 2\,, \end{aligned} \tag{3.2}$$

where $L_{\max}$ is the *minimum* number of layers required in order to recover $\Box$, recalling that:

$$L_i := \{y \in \mathcal{C} \mid y \prec x \text{ and } n\left(x,y\right) = i-1\}\,. \tag{3.3}$$

Introducing more layers is certainly possible but is equivalent to approximating a

second derivative in one-dimensional space with more than three points; it simply results in the non-uniqueness of coefficients [42]. Note that Aslanbeigi et al. define layers slightly differently, they start from $i = 0$ while we start from $i = 1$, i.e. in their definition of Eq. 3.3 the second condition is $n(x, y) = i - 2$.

The generalised form of the B operator applied to φ may be defined as [42]:

$$\rho^{-\frac{2}{d}} \left(B^{(d)}\varphi\right)(x) = a\varphi(x) + \sum_{i=1}^{L_{\max}} b_i \sum_{y \in I_i(x)} \varphi(y) \ , \tag{3.4}$$

where $\{a, b_i\}$ are dimensionless coefficients, I_i is the set of all the i-th neighbours to the past of x, and ρ is the density of sprinkled elements ($\rho \to \infty$ in the continuum limit). The coefficients are then fixed by requiring the operator to give the correct local limit in Minkowski $\mathbb{M}^d$ space. In flat space [41], and for the case with curvature [43, 44]:

$$\lim_{\rho\to\infty} \mathbb{E}\left(\mathbf{B}_\rho^{(d)}\varphi\right)(x) = \Box^{(d)}\varphi(x) - \frac{1}{2}R(x)\varphi(x) \ , \tag{3.5}$$

where $R(x)$ is the Ricci scalar evaluated at x (this term is only present in the limiting case with curvature), and $\mathbb{E}$ is the expectation value with respect to the Poisson sprinkling process which generated our causet $\mathcal{C}$. From now on we will use the notation $\langle ... \rangle$ to mean $\mathbb{E}$. A comprehensive list of coefficients was done by Dowker and Glaser in [43]. A few considerations must be made: first of all, the limit imposed is clearly equivalent to $l \to 0$ as $\rho = l^{-d}$; secondly we must use the expectation value of the discretised operator as $\left(\mathbf{B}_\rho^{(d)}\varphi\right)(x)$ is a random variable dependent on the $\mathcal{C}$ on which the discrete d'Alembertian was applied. Some conditions must also be imposed on $\varphi(x)$. The scalar field φ must be of compact support, and x must not be on the past boundary of this support. If this were the case, there would be unbounded calculations which result in divergences; this cutoff can be seen as a physical IR cutoff [40, 41]. The conditions on $\varphi(x)$ will be explicitly tested in Sec. 3.3.

Finally, numerical calculations show how fluctuations in $\left(\mathbf{B}_{\rho}^{(d)}\varphi\right)(x)$ appear in the continuum limit when the physical IR cutoff is fixed, such that the required $\Box^{(d)}\varphi(x)$ is not recovered [40]. A description of how these are damped is given by Sorkin in [41, 45] and by Benincasa and Dowker in [40].

The idea is to introduce an intermediate length scale over which the expression for the discrete d'Alembertian may be smeared out, all the while hoping that the averaging will suppress these fluctuations due to the law of large numbers. Therefore, a second discrete operator with a different length scale (l, equivalent to a different density ρ) but same form of expected value is sought: this operator is found by working backwards. Numerical simulations show that this modified version of the discretised d'Alembertian not only provides the expected continuum approximation, but also successfully damps fluctuations with the length scale (at increasing density) [40, 41].

For completeness, this modified discretised d'Alembertian operator in d dimensions is given by [42]:

$$\rho^{-\frac{2}{d}}\left(\tilde{B}^{(d)}\varphi\right)(x) = a\varphi(x) + \sum_{n=0}^{\infty}\tilde{b}_i \sum_{y\in I_i(x)}\varphi(y)\ , \tag{3.6}$$

where a is a dimensionless coefficient as before and $\tilde{b}_i$ is given by:

$$\tilde{b}_i = \epsilon(1-\epsilon)^i \sum_{j=0}^{L_{max}-1}\binom{i}{j}\frac{b_j\epsilon^j}{(1-\epsilon)^j}\ , \tag{3.7}$$

where $\epsilon = \tilde{\rho}/\rho$ and b_j are dimensionless coefficients as stated previously. Clearly, when $\tilde{\rho} = \rho$ the original discretised d'Alembertian, Eq. 3.4, is recovered. Also, here the binomial coefficients have been set to be zero by convention for $j > i$. By construction, the expected continuum limit of $\Box\varphi$ is recovered.

Four Dimensions

Due to there being different coefficients, or weightings, for the layers for different spacetime dimensions, it is helpful to explicitly state the required expressions using [44].

In particular, in four dimensions, the discrete d'Alembertian operator:

$$\left(B^{(4)}\varphi\right)(x) = \frac{4}{\sqrt{6}l^2}\left(-\varphi(x) + \left(\sum_{y\in L_1(x)} -9\sum_{y\in L_2(x)} +16\sum_{y\in L_3(x)} -8\sum_{y\in L_4(x)}\right)\varphi(y)\right) . \quad (3.8)$$

It is also useful to look at the expected value of the random variable formed when applying our operator to the causet $\mathcal{C}$:

$$\left\langle\left(\mathbf{B}^{(4)}_{\rho}\varphi\right)(x)\right\rangle = \frac{4}{\sqrt{6}}\sqrt{\rho}\left[-\varphi(x) + \rho\left(\int_{y\in J^-(x)} d^4y\sqrt{-g}\varphi(y)\left(1-9\xi+8\xi^2-\frac{4}{3}\xi^3\right)e^{-\xi}\right)\right] , \quad (3.9)$$

where $\xi = \rho V_{xy}$, and V_{xy} is the volume of the causal interval between x and y. It can be seen that this result holds by considering a Poisson distribution and using Eq. 2.14. This can be shown to respect the required behaviour in the limit.

3.2 The Benincasa-Dowker-Glaser Action

The Benincasa-Dowker-Glaser (BDG) causet action is a family of actions, one for each $d > 1$ [43, 46]. To construct this, the causet d'Alembertian operator is employed as defined (using the convention by Dowker and Glaser):

$$\left(B^{(d)}\varphi\right)(x) = \frac{1}{l^2}\left(\alpha_d\varphi(x) + \beta_d\sum_{i=1}^{n_d} C_i^{(d)}\sum_{y\in L_i}\varphi(y)\right) , \quad (3.10)$$

where $\{\alpha_d, \beta_d, C_i^{(d)}\}$ are constants defined by Dowker and Glaser in [43], n_d is the minimum number of required layers given by Eq. 3.2. Next, the scalar curvature of the causet is defined by applying the discretised operator to a constant scalar field $\varphi = -1$ at every x:

$$\begin{aligned} \mathcal{R}^{(d)}(x) &= B^{(d)}(-1)|_x \\ &= -\frac{2}{l^2}\left(\alpha_d + \beta_d \sum_{i=1}^{n_d} C_i^{(d)} N_i(x)\right), \end{aligned} \tag{3.11}$$

where $N_i(x) = |L_i(x)|$ is the cardinality of the i-th past layer of the causet with respect to x. When evaluating this over a causet faithfully embedded into a d-dimensional spacetime, the mean of the random variable will be $R(x)$ in the continuum limit.

The action is then defined by summing the causet scalar curvature $\mathcal{R}^{(d)}$ over the whole causet $\mathcal{C}$ [46]:

$$\begin{aligned} \frac{1}{\hbar}\mathcal{S}^{(d)}(\mathcal{C}) &= \frac{l^d}{2l_P^{d-2}} \sum_{x\in\mathcal{C}} \mathcal{R}^{(d)}(x) \\ &= -\left(\frac{l}{l_P}\right)^{d-2}\left(\alpha_d N + \beta_d \sum_{i=1}^{n_d} C_i^{(d)} N_i\right) \\ &= \zeta_d\left(N + \frac{\beta_d}{\alpha_d}\sum_{i=1}^{n_d} C_i^{(d)} N_i\right), \end{aligned} \tag{3.12}$$

where $\zeta_d = -\alpha_d\left(\frac{l}{l_P}\right)^{d-2}$, l_P is the Planck length, and l is the fundamental causet length scale.

Given the interest in the continuum behaviour, it is useful to determine the mean causet action:

$$\frac{1}{\hbar}\langle \boldsymbol{\mathcal{S}}_\rho^{(d)}(\mathcal{M})\rangle = \zeta_d\left(\langle \mathbf{N}_\rho(\mathcal{M})\rangle + \frac{\beta_d}{\alpha_d}\sum_{i=1}^{n_d} C_i^{(d)}\langle \mathbf{N}_{i,\rho}(\mathcal{M})\rangle\right). \tag{3.13}$$

The recovery of this expression will be shown explicitly. Let us recall the Poisson

distribution Eq. 2.14. The mean number of elements is straightforward; it is the probability of there being an element in a causet cell ΔV. Then, from the fact that in the continuum we replace $\Delta V \to d^d x\sqrt{-g}$ and so $\sum \to \int$. The mean number of elements is given by:

$$\langle \mathbf{N}_\rho (\mathcal{M}) \rangle = \rho \int_{\mathcal{M}} d^d x \sqrt{-g} \,. \tag{3.14}$$

The next term is the mean number of order intervals of order $(i+1)$. In this convention, we have included the bottom and top elements in the count. Thus, the probability of sprinkling an element at the bottom, x, and one at the top of this interval, y is required. These are simply given by the same expression as above, with the extra condition that $y \in J(x)$. Then, placing $(i-1)$ elements in between the two:

$$\langle \mathbf{N}_{i,\rho} (\mathcal{M}) \rangle = \rho^2 \iint\limits_{\substack{\mathcal{M}\times\mathcal{M} \\ y\in J^+(x)}} d^d x \sqrt{-g(x)}\, d^d y \sqrt{-g(y)} \frac{(\rho V_{xy})^{i-1}}{(i-1)!} e^{-\rho V_{xy}} \,, \tag{3.15}$$

where V_{xy} is the volume of the causal interval between x and y. Putting all this together, the averaged causet action becomes:

$$\begin{aligned} \frac{1}{\hbar}\langle \boldsymbol{\mathcal{S}}_\rho^{(d)} (\mathcal{M}) \rangle = \zeta_d \Bigg(& \rho \int_{\mathcal{M}} d^d x \sqrt{-g} \\ & + \frac{\beta_d}{\alpha_d} \sum_{i=1}^{n_d} C_i^{(d)} \rho^2 \iint\limits_{\substack{\mathcal{M}\times\mathcal{M} \\ y\in J^+(x)}} d^d x \sqrt{-g(x)}\, d^d y \sqrt{-g(y)} \frac{(\rho V_{xy})^{i-1}}{(i-1)!} e^{-\rho V_{xy}} \Bigg) \,. \end{aligned} \tag{3.16}$$

Four Dimensions

Similarly to how was stated for the causet d'Alembertian, in four dimensions, the action is:

$$\frac{1}{\hbar}\mathcal{S}^{(4)} (\mathcal{C}) = \frac{4}{\sqrt{6}} \frac{l^2}{l_P^2} \left(N - N_1 + 9N_2 - 16N_3 + 8N_4 \right) \,, \tag{3.17}$$

and the expected value:

$$\frac{1}{\hbar}\langle \boldsymbol{\mathcal{S}}_{\rho}^{(d)}\left(\mathcal{M}\right)\rangle = -\frac{4}{\sqrt{6}}\frac{\sqrt{\rho}}{l_P^2}\int\limits_{\mathcal{M}} dV_x \left(1-\rho\int\limits_{\mathcal{M}\cap J^+(x)} dV_y\left(1-9\rho V_{xy}+8\left(\rho V_{xy}\right)^2-\frac{4}{3}\left(\rho V_{xy}\right)^3\right)e^{-\rho V_{xy}}\right) . \quad (3.18)$$

Where we have chosen the normalisation such that we recover the Einstein-Hilbert action in the limit (up to possible boundary terms):

$$S_{\mathrm{EH}} = \frac{1}{2\kappa}\int_{\mathcal{M}} d^4x\,\sqrt{-g}R\,, \quad (3.19)$$

where $\kappa = \frac{8\pi G}{c^4}$.

3.3 The Infinite Slab

As previously mentioned, the scalar field must be of compact support. This most importantly means that a cutoff of the scalar field must be introduced when applying the causet d'Alembertian operator to a spacetime. As will be described in more detail in the next chapters (4, 5) and previously by Dowker in [47], the d'Alembertian operator acting on a constant scalar field, $\varphi = 1$, can be written as:

$$L_\rho(p) = \frac{4}{\sqrt{6}}\rho^{\frac{1}{2}}\left(1-\rho\mathcal{O}_4 I(p)\right)\,, \quad (3.20)$$

where we have:

$$I(p) = \int_{J^+(x)\cap\mathcal{M}} d^4q\sqrt{-g(q)}e^{-\rho V_{pq}}\,, \quad (3.21)$$

$$\mathcal{O}_4 = 1+9\rho\frac{d}{d\rho}+8\rho^2\frac{d^2}{d\rho^2}+\frac{4}{3}\rho^3\frac{d^3}{d\rho^3}\,, \quad (3.22)$$

where p and q are elements of the causet and $p \prec q$. We may notice that the operator's role is to kill off divergences. For the purposes of the upcoming example,

the flat case is considered, i.e. $g = -1$.

To portray the importance of requiring a cutoff (φ to be of compact support), consider a four-dimensional slab that stretches off to infinity in the positive x^μ direction, i.e. half of infinite $\mathbb{M}^4$. Then two points are placed, p and q, and it is imposed that the latter must be within the future light cone of the former, i.e. $q \in J^+(p)$, see Fig. 3.1. Then, due to spatial translation invariance, it is possible to choose p to be positioned at $(p_0, 0, 0, 0)$ without loss of generality.

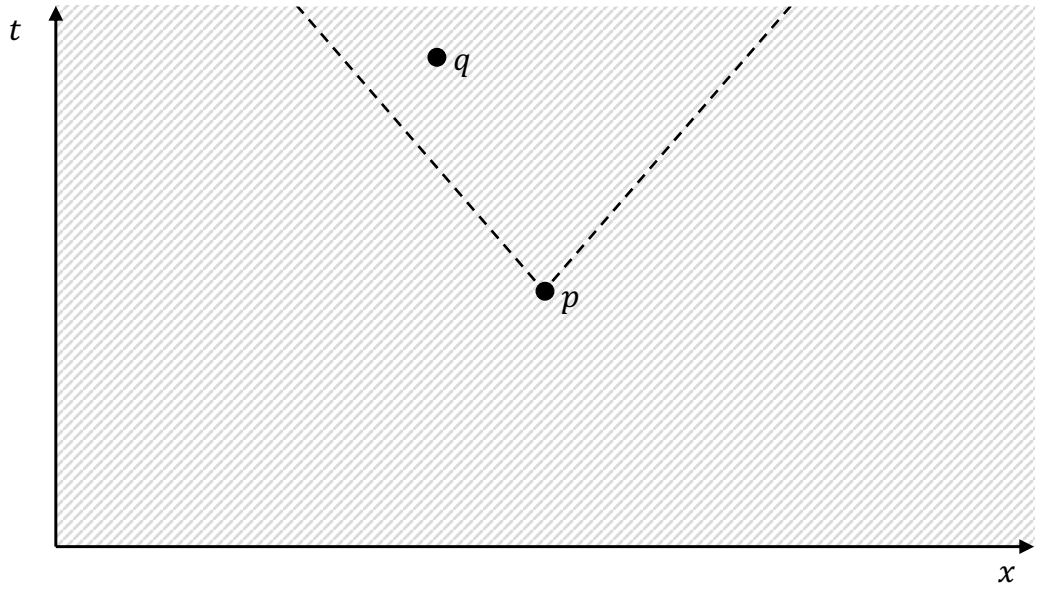

Figure 3.1: A section of the infinite slab (shaded), with the y and z spatial dimensions suppressed, showing the position of points p and q. The integral is performed over the region in the slab in the causal future of p, shown by the dashed line.

To compute the integral (Eq. 3.21), radial null coordinates (u, v, θ, ϕ) centred on p are a convenient choice. First, a coordinate transformation is performed by defining a new set of coordinates for which p is at the origin, $\{x^\mu\} \to \{z^\mu\}$. Then, the radial null coordinates are defined as:

$$u = \frac{1}{\sqrt{2}}\left(z^0 - \|z^i\|\right) , \qquad v = \frac{1}{\sqrt{2}}\left(z^0 + \|z^i\|\right) , \tag{3.23}$$

together with polar coordinates ϕ and θ described in the usual way. The integration

measure becomes:

$$d^4q = \|J\|\, du\, dv\, d\theta\, d\phi = \frac{1}{2}(v-u)^2 \sin\theta\, du\, dv\, d\theta\, d\phi\,, \tag{3.24}$$

where $\|J\|$ is the modulus of the determinant of the Jacobian matrix of the transformation. As limits of integration, having invoked spherical symmetry:

$$\begin{aligned} v \in [u, \infty]\ , \qquad u \in [0, \infty]\ , \\ \theta \in [0, \pi]\ , \qquad \phi \in [0, 2\pi]\ . \end{aligned} \tag{3.25}$$

So the integral becomes (recalling the sla is embedded in flat space):

$$I(p) = \int_0^\infty du \int_u^\infty dv \int_0^\pi d\theta \int_0^{2\pi} d\phi\, \frac{1}{2}(v-u)^2 \sin\theta\, e^{-\rho\frac{\pi}{6}v^2u^2}\,, \tag{3.26}$$

where the calculations for the volume of the interval V_{pq} are used (shown in detail in Sec. 4.4).

The v, θ, ϕ integrals can be computationally integrated, for instance using Mathematica, while the u integral cannot. To make Mathematica compute this last integral, we may employ a trick. It can be noticed that u is independent of ρ, and so one can differentiate with respect to ρ under the integral sign. Thus, the operator $\mathcal{O}_4$ is commuted with the integral. Having done this, we give it back to Mathematica, which is now able to fully compute the integral analytically. Evaluating the u integral then gives:

$$\mathcal{O}_4 I(p) = -\frac{1}{\rho}\,, \tag{3.27}$$

putting it all together:

$$L_\rho(p) = 4\sqrt{\frac{2}{3}}\sqrt{\rho}\,, \tag{3.28}$$

which in the continuum limit clearly diverges in the expected fashion:

$$\lim_{\rho\to\infty} L_\rho\,(p) \to \infty\,. \tag{3.29}$$

This divergence is avoided by imposing a cutoff on the integration, that is, by requiring the scalar field φ to be of compact support.

Chapter 4

The Benincasa-Dowker Conjecture

Following considerations made in chapter 3, it has been seen that the continuum limit of the Benincasa-Dowker-Glaser action gives the Einstein-Hilbert action up to some boundary terms. Benincasa and Dowker [46] subsequently suggested, in the shape of a conjecture, the form and origin of these boundary terms for a globally hyperbolic spacetime.

4.1 The Conjecture

Consider a d-dimensional globally hyperbolic Lorentzian spacetime $(\mathcal{M}, g)$ of finite volume with a causal set $\mathcal{C}$ sprinkled in it at density ρ. The causet action then gives rise to a random variable $\boldsymbol{\mathcal{S}}_\rho(\mathcal{M})$ that in the continuum tends to the Einstein-Hilbert action plus boundary terms. The boundaries of $\mathcal{M}$ are required to be achronal, such that $\partial\mathcal{M} := \Sigma_- \cup \Sigma_+$ where $\Sigma_\pm$ can be null, spacelike, or both but not timelike. Then, the conjecture by Benincasa and Dowker [46].

Conjecture 4.1 (Benincasa-Dowker Conjecture)**.**

$$\lim_{\rho\to\infty} \frac{1}{\hbar}\langle \boldsymbol{\mathcal{S}}_\rho^{(d)}(\mathcal{M})\rangle = \frac{1}{l_p^{d-2}}\int_{\mathcal{M}} d^dx\sqrt{-g}\frac{R}{2} + \frac{1}{l_p^{d-2}}\,Vol_{d-2}(J)\ , \tag{4.1}$$

where R is the Ricci curvature scalar, $J := \Sigma_- \cap \Sigma_+$ is the "joint" and $Vol_{d-2}(J)$ is its volume.

The justification presented by Benincasa [46] and Dowker [47] is as follows. Let us start by recalling that all that has been done in chapter 3 is based on the *retarded* convention; that is, the layers used are sets of elements which precede x, the *past* layers. Alternatively, one could equally as well have chosen the advanced convention and recovered the same results, using the *future* layers. The order can be reversed, and now x is succeeded by the employed layers (they are to its future). However, the action is the same: it is invariant under this order reversal.

To see the conjecture, let us then examine the retarded version. For a large enough ρ, and given that x is not on the past boundary of $\mathcal{M}$, there will be enough points to the past of x such that the Ricci curvature scalar can be recovered in the continuum limit of $\langle \boldsymbol{\mathcal{R}}_{\rho}^{(d)}(x) \rangle$. This can be justified by noticing that there will be enough elements for all required layers to exist and achieve the necessary cancellations. In particular, we are interested in the fact that this works for an x on the future boundary of $\mathcal{M}$ but *not* on the past boundary, where only the Einstein-Hilbert contribution is expected. The analogous argument can be made for the advanced version: this works for an x on the past boundary of $\mathcal{M}$ but *not* on its future boundary, where again only the Einstein-Hilbert contribution is to be expected.

Clearly, in the union of these two sets, those points which appear both on the future and past boundaries of $\mathcal{M}$ have not been included. These make up a special set known as the "joint" (see Sec. 4.3), where elements have no past nor future: their contribution will not be the Einstein-Hilbert term but something else.

4.2 The Order of Integration

The expression for the left hand side of the conjecture Eq. 3.16 can be simplified into a form which will turn out to be very useful. In order to do this, the order of integration must be decided, as choosing to do the y or x integral first is equivalent

to selecting the advanced or retarded convention, respectively. We will choose the advanced version, as done by Dowker in [47].

Some considerations will be made in order to make the integration more manageable. These have already been seen in part in Sec. 3.3 in the form of the differential ρ operator and the discretised d'Alembertian integral.

It may be noticed how the $\langle \mathbf{N}_{i,\rho}(\mathcal{M})\rangle$, Eq. 3.15 can be rewritten using the mean number of links $\langle \mathbf{N}_{\text{Links},\rho}(\mathcal{M})\rangle$:

$$\langle \mathbf{N}_{\text{Links},\rho}(\mathcal{M})\rangle = \langle \mathbf{N}_{1,\rho}(\mathcal{M})\rangle = \rho^2 \iint\limits_{\substack{\mathcal{M}\times\mathcal{M}\\ y\in J^+(x)}} dV_x\, dV_y\, e^{-\rho V_{xy}}\,. \tag{4.2}$$

Where it has been used that this is non-other than an order interval of order two, $\langle \mathbf{N}_{1,\rho}(\mathcal{M})\rangle$. The expected value for the order $i+1$ interval is then given by:

$$\langle \mathbf{N}_{i,\rho}(\mathcal{M})\rangle = \rho^2 \frac{\rho^{i-1}}{(1-1)!}\left(-\frac{d}{d\rho}\right)^{i-1}\left[\rho^{-2}\langle \mathbf{N}_{1,\rho}(\mathcal{M})\rangle\right]\,, \tag{4.3}$$

which may then be substituted back into the mean causet action. This may be rewritten in a simplified manner using some newly defined quantities:

$$\frac{1}{\hbar}\langle \boldsymbol{\mathcal{S}}^{(d)}_{\rho}(\mathcal{M})\rangle = \frac{1}{l_P^{d-2}}\int_{\mathcal{M}} dV_x\, \mathcal{L}_\rho(x)\,, \tag{4.4}$$

where:

$$\mathcal{L}_\rho(x) := -\rho^{\frac{d}{2}}\left(\alpha_d + \rho\beta_d \int_{\mathcal{M}\cap J^+(x)} dV_y\, \mathcal{O}_4 e^{-\rho V_{xy}}\right)\,, \tag{4.5}$$

$$\mathcal{O}_d := \sum_{i=1}^{n_d} \frac{C_i^{(d)}}{(i-1)!}\rho^{i-1}\left(-\frac{d}{d\rho}\right)^{i-1}\,, \tag{4.6}$$

and the constants defined by Dowker and Glaser [43, 44] $\{\alpha_d, \beta_d, C_i^{(d)}\}$ have again been used. This not only makes the expression much easier to deal with, it also shows how the operator's role removes certain divergences by annihilating certain powers of ρ.

Four Dimensions

It will be beneficial to note down the above expressions in four dimensions:

$$\frac{1}{\hbar}\langle \boldsymbol{\mathcal{S}}^{(4)}_{\rho}(\mathcal{M})\rangle = \frac{1}{l_P^2}\int_{\mathcal{M}} dV_x\, \mathcal{L}_\rho(x)\ , \tag{4.7}$$

and:

$$\mathcal{L}_\rho(x) := -\frac{4}{\sqrt{6}}\sqrt{\rho}\left(1-\rho\mathcal{O}_4\int_{\mathcal{M}\cap J^+(x)} dV_y\, e^{-\rho V_{xy}}\right)\ , \tag{4.8}$$

$$\mathcal{O}_4 = 1 + 9\rho\frac{d}{d\rho} + 8\rho^2\frac{d^2}{d\rho^2} + \frac{4}{3}\rho^3\frac{d^3}{d\rho^3}\,. \tag{4.9}$$

where we have commuted the operator with the integral as the region $\mathcal{M}\cap J^+(x)$ is independent of ρ.

4.3 The Joint

The joint term in the conjecture is a boundary term; it arises due to divergences appearing on the boundaries. It is defined to be the intersection between the future and past boundaries of the spacetime:

$$J := \Sigma_- \cap \Sigma_+\,. \tag{4.10}$$

These boundaries can be defined by what follows. We start by recalling Cauchy surfaces and imposing a notion of "global hyperbolicity" on the spacetime. These can be defined as:

Definition 4.1. A *Cauchy surface*, Σ, is an achronal spacelike hypersurface such that every causal curve may only intersect it once. Its domain of dependence is the entire manifold.

Definition 4.2. A *globally hyperbolic* spacetime is one which contains a Cauchy surface, Σ.

The information on a Cauchy surface can be thought of as the "initial conditions" of a deterministic system. The implications of this requirement are massive: by providing appropriate information on Σ, one may solve the theory completely, as the entire manifold lies in its domain of dependence [48]. These conditions ensure that, for the purposes of this conjecture, all boundaries are either null or spacelike. Also, it will be useful to note that a boundary is of codimension one while the joint is of codimension two; explaining the Vol_{d-2} term of the conjecture. Fig. 4.1 contains some examples of hyperbolic spacetimes.

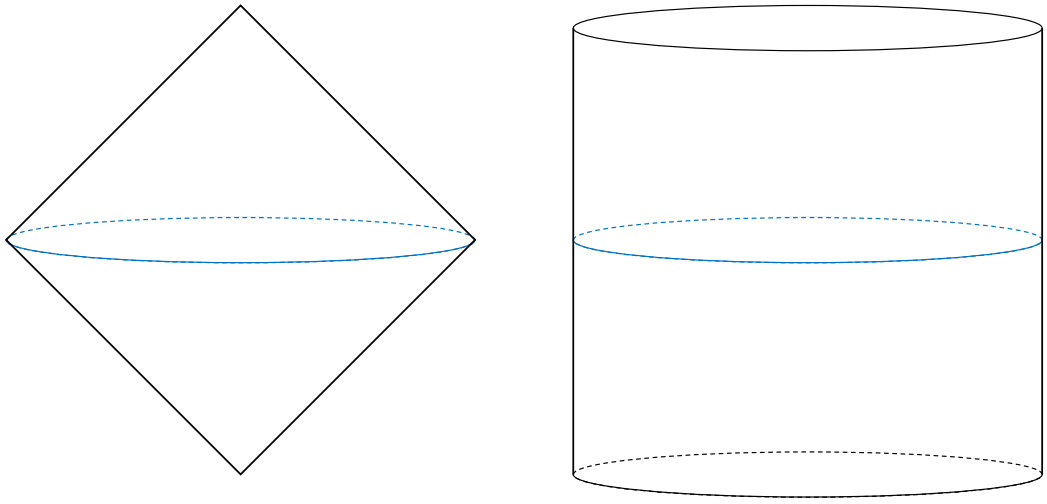

Figure 4.1: Cauchy surfaces (blue) in different spacetimes. (a) The four-dimensional interval, the Cauchy surface and null boundaries are shown; the Cauchy surface is also the joint. (b) The two-dimensional slab with vertical spacelike boundaries and showing one of the possible Cauchy surfaces (any horizontal circle drawn will be a Cauchy surface), this spacetime does not contain a joint.

Strictly speaking, the diagrams in Fig. 4.1 are not Lorentzian manifolds as the boundaries have been included:

Definition 4.3. A *past* (*future*) boundary is an area from which past (future) directed curves may leave a spacetime.

The joint will then be where these two meet (if indeed they do); Fig 4.1 gives an

example of each case.

From all of this, we understand why, how, and where these joint terms appear. It can then be proven that the contribution will be the codimension-2 volume of the intersection of the $(d-1)$-surfaces: a $(d-2)$-sphere of radius $\frac{\tau}{2}$, where τ is the proper time separating x and y [46]. Spacetimes with curvature will, as usual, have higher-order corrections.

4.4 The Interval

Another aspect of the conjecture of interest to this work is the volume V_{pq}, that is, the volume of the causal interval between p and q. The Alexandrov interval between two points is defined as:

$$A\left(p,q\right)=J^{+}\left(p\right)\cap J^{-}\left(q\right)\ , \tag{4.11}$$

for $p\prec q$, colloquially, this is also known as a causal diamond.

In Minkowski spacetime $\mathbb{M}^d$, there exists a unique timelike geodesic between two points with proper length τ. Thus, the volume will be a function of τ. To see this, consider two points and perform a Lorentz boost such that they are at the same spatial coordinates but different time coordinate. Clearly, their spacetime position difference will be their proper time τ. Using that it is a Lorentz invariant quantity, we may show the volume will be dependent solely on τ.

Calculating this volume is relatively straightforward; a spacetime integral can be performed over a cone [49]:

$$V_{pq}^{(d)}=\int_{J^{+}(p)\cap J^{-}(q)}d^{d}x\,\sqrt{-g}\,. \tag{4.12}$$

For the flat case, it is a known function of τ. However, for the case with curvature, a series expansion is required. Various methods are explained in the literature [27, 49],

and they all have the same final result up to a sign. In four dimensions, up to $\mathcal{O}(\tau^3)$, there is the expression for the volume of the Alexandrov interval in Riemann normal coordinates:

$$V_{pq}^{(4)} = \frac{\pi}{24}\tau^4 \left[1 + \frac{1}{180}R(0) + \frac{1}{30}\tau^2 R_{00}(0) + \mathcal{O}\left(\tau^3\right)\right], \tag{4.13}$$

where the Ricci scalar R and the time-time component of the Ricci tensor R_{00} are evaluated at the origin.

4.5 The Evidence

Although there is yet to be a formal proof for this conjecture, numerous pieces of evidence are available in the literature. All follow a similar approach: a globally hyperbolic manifold is taken, and the mean of the random discrete action is calculated. Many are in flat two-dimensional spacetime: see the flat causal interval [46]; the null triangle, the null cylinder, the slab [50]. An extension with the addition of a specific conformally flat metric was done for both two- and four-dimensional spacetimes by Dowker [47] and Bhatnagar [51]. An extension to all dimensions and arbitrary curvature for the causal interval can also be found [52, 53]; some examples, though, have been done in a neighbourhood in which Riemann normal coordinates apply.

Chapter 5

The Four-Dimensional Flat Slab

In this chapter, evidence will be added to that already present in the literature. By using a combination of analytical and numerical methods, it will be shown how the four-dimensional slab does indeed respect conjecture 4.1 in the flat case. Note that from here to the end of this chapter, the superscript $^{(4)}$ above the action will be dropped, as the problem implies $d = 4$.

5.1 The Geometry

First of all, one must decide how the slab is to be defined. Let us choose a slab of height T in the time dimension and width L in all three spatial dimensions, described by coordinates $\{x^\mu\}$, see Fig. 5.1.

In constructing this manifold, we identify opposite sides of the spatial boundaries with each other (antipodal identification); that is, a particle moving eastwards in the x^1 direction will reach $x^1 = L$ and then reappear at $x^1 = 0$. Topologically this is an $S^1 \times S^1 \times S^1 \times R$; we may think of it as a four-dimensional cylinder, or without the time axis, just a 3-torus, T^3. This identification imposes spatial translation invariance without loss of generality, as the manifold looks the same wherever we are along the spatial axes, thus significantly facilitating the problem at hand. Precisely, it ensures that the outer integral can be performed only over the

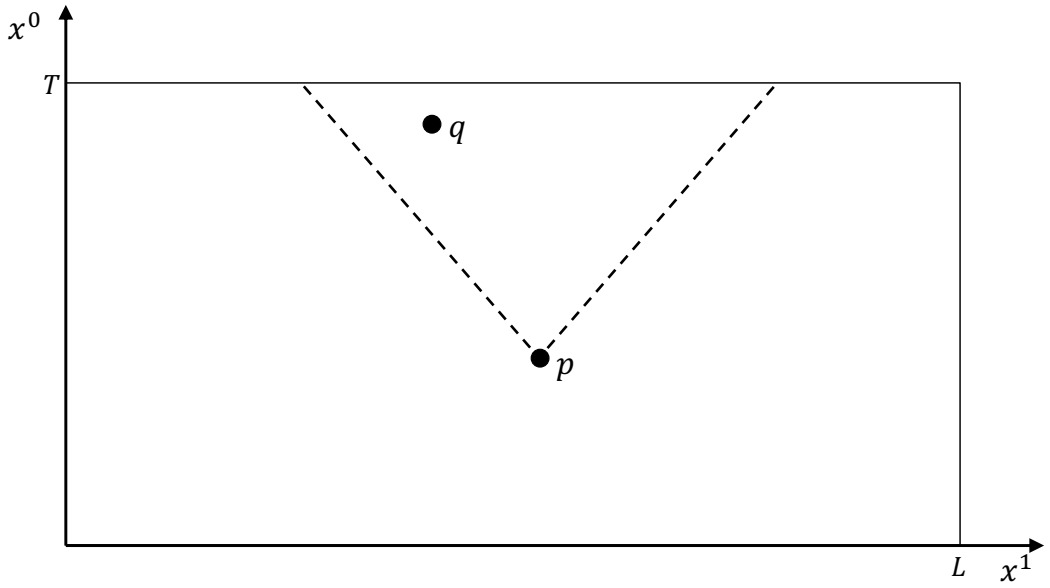

Figure 5.1: The four-dimensional slab, with the x^2 and x^3 spatial dimensions suppressed, showing the position of points p and q. The first integral is performed over the dashed region in the slab (the causal future of p), while the second is over the full manifold.

time coordinate, p^0, as the integrand will be independent of p^i.

This notion of spatial translation invariance allows us to fix the spatial coordinates of p to whatever is most useful to us. We may do this simply by translating the point, but always ensuring that the time coordinate, p^0, remains untouched. For the set of calculations and examples that follow, we will always assume $p = (p^0, 0, 0, 0)$ unless explicitly stated otherwise. On the other hand, the only condition made on q is that it must lie in the causal future of p, as stated in the conjecture.

Wrap-Around

Next, in deciding how T and L should be related (if at all), we will introduce the notion of "wrap-around". We may recall from the previous chapter that the interval between points p and q appears within the integrand. We must then picture this on our manifold to determine over which areas to integrate. It turns out that the relationship we choose between the height and width of our slab will either greatly

complicate, or simplify, the calculation. For simplicity, these considerations are made in $(1+1)$-dimensional space, but the arguments apply identically to our case of $(3+1)$ dimensions.

Let us first consider the two-dimensional *tall-thin* slab ($T \gg L$):

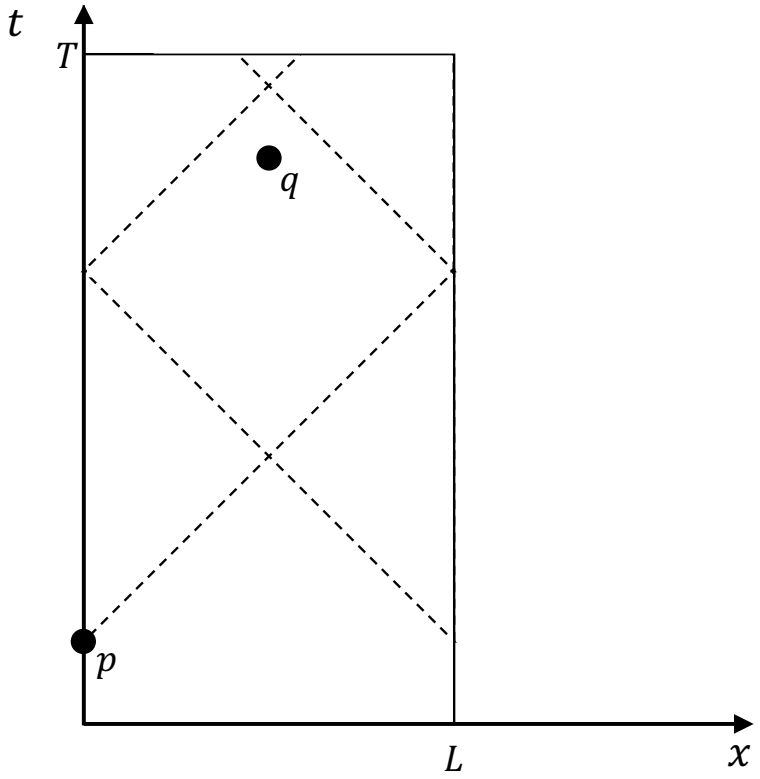

Figure 5.2: The tall-thin slab ($T \gg L$) is pictured in two dimensions. The dotted line represents the boundary of the causal future of point p.

Clearly, the interval over which we must compute the first integral is not immediately obvious: there are many patches and areas of overlap which would complicate the calculations. While attempting to compute this integral, the following concerns arise:

1. We must calculate each portion, and so volume, of the integral separately;

2. We must consider all possible positions of q with respect to p as these will have different interval patterns (some of which will be straightforward), and so will have to be done on a case-by-case basis.

Nevertheless, we should note that these two problems do not increase the actual difficulty of the problem: they just make it much more tedious to do.

Next, the *short-fat* slab ($T \ll L$):

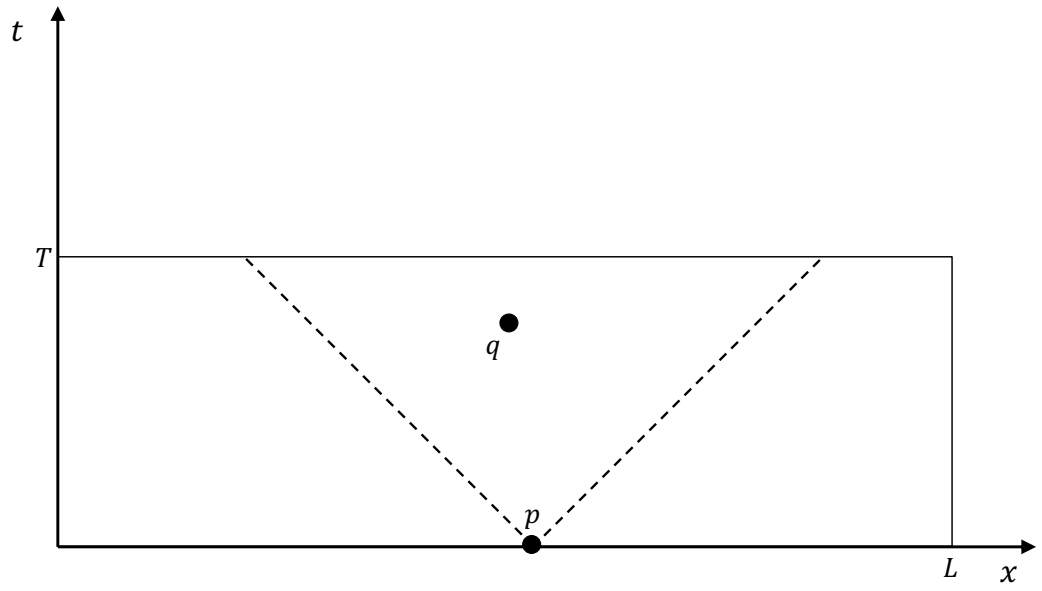

Figure 5.3: The short-fat slab ($T \ll L$) is pictured in two dimensions. The dotted line represents the boundary of the causal future of point p.

Here, we have translated p to a position more suitable to illustrate this example. Noticeably, the interval over which the first integral must be computed is now obvious to see: it is in one clear piece without any tricky bits or overlaps. This applies even when the future cone is at its largest (at $p^0 = 0$), as shown in Fig 5.3.

Evidently, the second relation between the height and width will make the problem much more approachable, but now begs the question: may we impose such a condition? The answer is yes, as we are only interested in the continuum limit where $\rho \to \infty$. While the contribution from the two manifolds will clearly differ, in the limit case, two considerations allow us to do this. First of all, they will have the same dependence on ρ, so the limit will be identical; and secondly, the variables we are using to change the shape of this manifold, T and L, are independent of ρ, and so, when we take the limit, we will achieve the same result.

5.2 The Conjectured Result

The conjectured solution involves the Einstein-Hilbert term and the joint term. Starting from the Einstein-Hilbert term, we may see:

$$S_{\text{EH}} = \frac{1}{\kappa}\int_{\mathcal{M}} d^d p\,\sqrt{-g}\frac{R}{2} = 0\,, \tag{5.1}$$

having used that $R = 0$ in the flat case. The joint term is similarly trivial, there is no intersection between the future boundary $t = T$ and past boundary $t = 0$ of the slab, and so this too is zero. We then expect:

$$\lim_{\rho\to\infty}\frac{1}{\hbar}\langle \boldsymbol{\mathcal{S}}_\rho\left(\mathcal{M}\right)\rangle = 0\,. \tag{5.2}$$

5.3 The Inner Integral

First of all, we should note that some calculations will resemble those done in section 3.3. Let us start by considering the inner integral of Eq. 4.8, the one over p's causal future $J^+\left(p\right)$ shown by the dotted line in Fig. 5.1:

$$I\left(p\right) = \int_{J^+(p)} d^4q\, e^{-\rho V_{pq}}\,. \tag{5.3}$$

To evaluate this integral, we may notice how the integral element is independent of the density ρ, so we may commute the differential operator $\mathcal{O}_4$ into the integral:

$$\mathcal{O}_4 I\left(p\right) = \int_{J^+(p)} d^4q\,\left(1 - 9\rho V_{pq} + 8\left(\rho V_{pq}\right)^2 - \frac{4}{3}\left(\rho V_{pq}\right)^3\right) e^{-\rho V_{pq}}\,, \tag{5.4}$$

where we have applied Eq. 4.9 to our previous expression and have that $V_{pq} = \frac{\pi}{24}\tau^4$ with τ being the proper time between p and q.

By recalling that we may place p at $(p^0, 0, 0, 0)$ without loss of generality, we may define a new height, $T_p = T - p^0$, as the distance between p and the top of the slab.

Furthermore, we may notice that due to the geometry of the slab and the fact that the dotted lines (the boundaries of $J^+(p)$) in Fig. 5.1 are null lines; we are able to make a convenient coordinate transformation to radial null coordinates (u, v, θ, ϕ) centred at p. This can all be seen in Fig. 5.4.

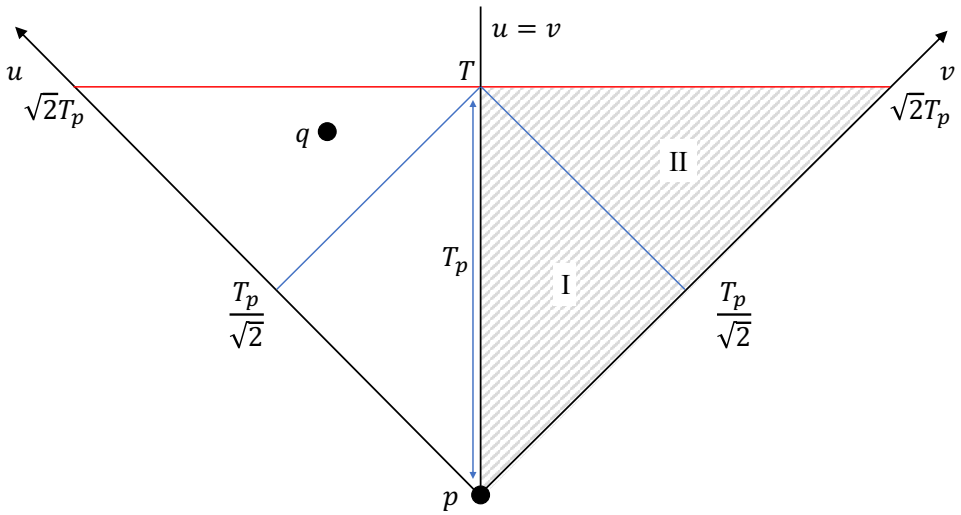

Figure 5.4: The future cone of p, specifically the construction for the integral in $I(p)$ using radial null coordinates where we may think of each point on the diagram as a 2-sphere, S^2. The u and v integrals must be computed over the shaded areas, where $T_p = T - p^0$. Blue lines are construction lines, while the red line is the top of the slab, $t = T$. We also have that the u and v lines are the boundary of $J^+(p)$.

Explicitly, the full coordinate transformation takes place in three steps. The first coordinate transformation, $\{x^0\} \to \{z^\mu\}$, consists of a time translation to centre at p:

$$z^0 = x^0 - p^0\,, \qquad z^i = x^i\,. \tag{5.5}$$

Next, defining spherical polar coordinates (t, r, θ, ϕ):

$$t = z^0\,, \qquad r = \|z^i\|\,, \tag{5.6}$$

with the polar coordinates θ and ϕ defined in the usual way. The integration measure

becomes:

$$d^4q = \|J_{\text{Spherical}}\|\, dt\, dr\, d\theta\, d\phi = r^2 \sin\theta\, dt\, dr\, d\theta\, d\phi\,, \tag{5.7}$$

where $\|J_{\text{Spherical}}\|$ is the modulus of the Jacobian for the transformation from $\{z^\mu\}$ to spherical coordinates. Then, define radial null coordinates as:

$$u = \frac{1}{\sqrt{2}}(t - r)\ , \qquad v = \frac{1}{\sqrt{2}}(t + r)\ , \tag{5.8}$$

with the polar coordinates being kept as they were. The integration measure then:

$$d^4q = \frac{1}{2}(v - u)^2 \sin\theta\, du\, dv\, d\theta\, d\phi\,, \tag{5.9}$$

where we used that $\|J_{\text{Null}}\| = 1$.

Finally, we also need an expression for the volume in radial null coordinates. We start from the expression for the volume $V_{pq} = \frac{\pi}{6}\tau^4$, so we now only need the proper time between p and q in these coordinates. Starting from:

$$\begin{aligned}
\tau^2 &= (z^0)^2 - (z^1)^2 - (z^2)^2 - (z^3)^2 && (5.10)\\
&= t^2 - r^2 && (5.11)\\
&= \frac{1}{2}(v + u)^2 - \frac{1}{2}(v - u)^2 && (5.12)\\
&= 2uv\,. && (5.13)
\end{aligned}$$

Thus, the volume of the causal interval between p and q is:

$$V_{pq} = \frac{\pi}{6}u^2v^2\,. \tag{5.14}$$

The u Integral

As we are working in four dimensions (two of which are polar angles), we must only consider the grey shaded area in Fig. 5.1 for integration over u and v. Which, for

reasons that will soon become apparent, can conveniently be split into two regions, I and II. Respectively, their bounds of integration are:

$$\text{I:} \qquad u \in [0, v] \ , \qquad v \in \left[0, \frac{T_p}{\sqrt{2}}\right] \ , \tag{5.15}$$

$$\text{II:} \qquad u \in \left[0, \sqrt{2}T_p - v\right] \ , \qquad v \in \left[\frac{T_p}{\sqrt{2}}, \sqrt{2}T_p\right] \ , \tag{5.16}$$

and they have the same bounds for the polar coordinates:

$$\text{I, II:} \qquad \theta \in [0, \pi] \ , \qquad \phi \in [0, 2\pi] \ , \tag{5.17}$$

these always integrate into a factor of 4π as the integrand is independent of both θ and ϕ; we will assume this has been done.

Putting all of this together, we may separate Eq. 5.4 into two terms as:

$$\mathcal{O}_4 I\left(p\right) = I_{\text{I}}\left(p\right) + I_{\text{II}}\left(p\right) \ , \tag{5.18}$$

where we now have absorbed $\mathcal{O}_4$ into the newly defined integrals:

$$I_{\text{I}}\left(p\right) = 4\pi \int_0^{\frac{T_p}{\sqrt{2}}} dv \int_0^v du \, \frac{1}{2}\left(v-u\right)^2 \left(1 - 9\rho\left(\frac{\pi}{6}u^2v^2\right) + 8\rho^2\left(\frac{\pi}{6}u^2v^2\right)^2 - \frac{4}{3}\rho^3\left(\frac{\pi}{6}u^2v^2\right)^3\right) e^{-\rho\frac{\pi}{6}u^2v^2} \ , \tag{5.19}$$

$$I_{\text{II}}\left(p\right) = 4\pi \int_{\frac{T_p}{\sqrt{2}}}^{\sqrt{2}T_p} dv \int_0^{\sqrt{2}T_p - v} du \, \frac{1}{2}\left(v-u\right)^2 \left(1 - 9\rho\left(\frac{\pi}{6}u^2v^2\right) + 8\rho^2\left(\frac{\pi}{6}u^2v^2\right)^2 - \frac{4}{3}\rho^3\left(\frac{\pi}{6}u^2v^2\right)^3\right) e^{-\rho\frac{\pi}{6}u^2v^2} \ . \tag{5.20}$$

Now, turning to Mathematica to evaluate these integrals, we will do one part at

a time and one term at a time. We perform the u integrals:

$$I_{\mathrm{I}}(p) = \frac{2\pi}{3}\int_0^{\frac{T_p}{\sqrt{2}}} dv\, v^3 e^{-\rho\frac{\pi}{6}v^4}\,, \tag{5.21}$$

$$\begin{aligned} I_{\mathrm{II}}(p) =& \frac{\pi}{27}\int_{\frac{T_p}{\sqrt{2}}}^{\sqrt{2}T_p} dv\, \left(\sqrt{2}T_p - v\right) e^{-\rho\frac{\pi}{6}v^2\left(v-\sqrt{2}T_p\right)^2} \\ & \Big(36T_p^2 - 90\sqrt{2}T_p v + \left(126 - 60\pi\rho T_p^4\right)v^2 + 192\sqrt{2}\pi\rho T_p^3 v^3 \\ & + \left(8\pi^2\rho^2 T_p^6 - 438\pi\rho T_p^2\right)v^4 + \left(210\sqrt{2}\pi\rho T_p - 32\sqrt{2}\pi^2\rho^2 T_p^5\right)v^5 \\ & + \left(104\pi^2\rho^2 T_p^4 - 72\pi\rho\right)v^6 - 88\sqrt{2}\pi^2\rho^2 T_p^3 v^7 + 82\pi^2\rho^2 T_p^2 v^8 \\ & -20\sqrt{2}\pi^2\rho^2 T_p v^9 + 4\pi^2\rho^2 v^{10}\Big)\,. \end{aligned} \tag{5.22}$$

The v Integral: Part One

We then perform the v integrals:

$$I_{\mathrm{I}}(p) = \frac{1 - e^{-\rho\frac{\pi}{24}T_p^4}}{\rho}\,, \tag{5.23}$$

and we notice Mathematica is unable to perform the v integral for I_{II}. However, we do not believe this to be a case where the conjecture is invalid. We believe the error is due to Mathematica simply not being able to analytically perform integrals of the form:

$$\int_b^a f(v,\rho)\, e^{-\rho h(v)}\,, \tag{5.24}$$

where $f(v,\rho)$ is an n-th order polynomial in v ($n > 0$), and $h(v)$ is a fourth order polynomial. We may justify this belief by recalling that the upwards pointing triangle was shown to respect the conjecture [51], and this area of integration is similar to the downwards pointing triangle. As we are in flat space, we expect the same final answer from the two triangles: they just differ by the order of integration and else have identical geometry.

A Slight Deviation: ***The Continuum Limit of a 4-Dimensional Causal Set Scalar d'Alembertian***

In order to perform the v integral in I_{II}, we make use of the result in a paper by Belenchia, Benincasa, and Dowker [3]. We first verify the results for this geometry by adapting Fig. 1 on page 6 of the original paper [3], see Fig. 5.5. There are some considerations we must make:

- We have a hard cutoff at the top of the slab for the support of the scalar field, φ.
- We have a constant scalar field, $\varphi = 1$, while the paper does not.
- The area of integration $\mathcal{W} = \sum_i^3 W_i$ must fully contain the support of φ.
- We choose $a \to 0$ and $\rho \to \infty$ such that $\rho a^4 \to \infty$ to have that $e^{-\rho a^4}$ so $a \sim \rho^{-1/8}$.

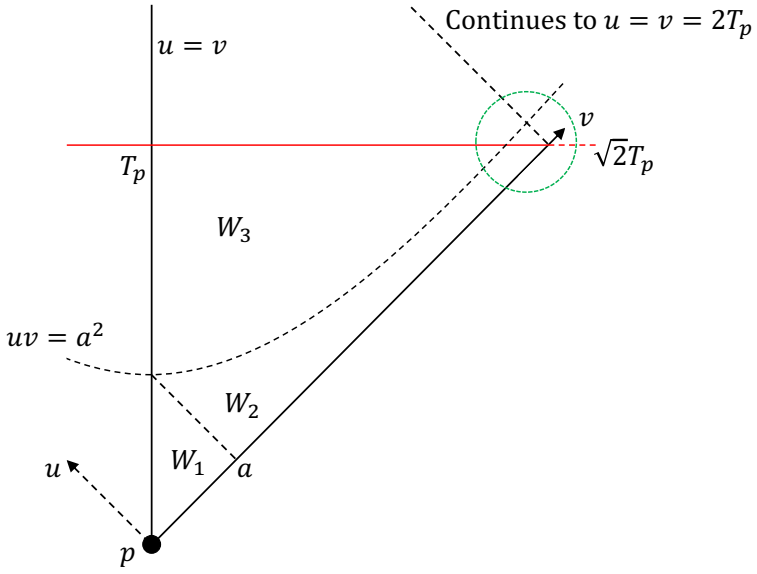

Figure 5.5: A reproduction of Fig. 1, page 6, of [3], with adjustments made according to Fig. 5.4. We have separated the regions with a parabola $uv = a^2$. The general cutoff on the scalar field has been substituted with a hard cutoff (red line), and an area of interest is circled in green in the top right region of the diagram, see Fig. 5.6.

The paper states that:

$$L_\rho(p) = \frac{4}{\sqrt{6}}\sqrt{\rho}\left(-1 + \rho\sum_i^3 R_i(p)\right), \tag{5.25}$$

goes to zero in the limit $\rho \to \infty$, where we have:

$$R_i(p) = \int_{W_i} d^4q \left(1 - 9\rho V + 8(\rho V)^2 - \frac{4}{3}(\rho V)^3\right) e^{-\rho V}, \tag{5.26}$$

the bounds of integration over the null coordinates are:

$$W_1: \qquad u \in [0, v], \qquad v \in [0, a], \tag{5.27}$$

$$W_2: \qquad u \in \left[0, \frac{a^2}{v}\right], \qquad v \in \left[a, \sqrt{2}T_p\right], \tag{5.28}$$

and:

$$W_3: \qquad u \in \left[\frac{a^2}{v}, v\right], \qquad v \in \left[a, \sqrt{2}T_p\right]. \tag{5.29}$$

We will verify the result for our slab, starting with R_3. Using similar arguments, we can see that V is bounded from zero in W_3 and so clearly $V \geq V_{\min} = \frac{\pi}{6}a^4$, this means:

$$e^{-\rho V_{\min}} \geq e^{-\rho V}. \tag{5.30}$$

Then we may see:

$$|R_3(p)| \leq e^{-\rho V_{\min}} \int_{W_3} d^4q \left|1 - 9\rho V + 8(\rho V)^2 - \frac{4}{3}(\rho V)^3\right|, \tag{5.31}$$

which in the limit $\rho \to \infty$ goes to zero much faster than any negative power term of ρ; we know these as "exponentially small" terms [3].

Next, we consider region W_1, which we note was similarly done by Dowker [47],

and is also very alike to I_{I} done previously. We do this explicitly using Mathematica:

$$R_1(p) = 4\pi \int_0^a dv \int_0^v du \, \frac{1}{2}(v-u)^2 \left(1 - 9\rho + 8(\rho V)^2 - \frac{4}{3}(\rho V)^3\right) e^{-\rho V}, \quad (5.32)$$

with $V = \frac{\pi}{6}u^2v^2$ and having already performed the integration over the polar coordinates. Mathematica is able to perform both integrals:

$$R_1(p) = \frac{1 - e^{-\rho\frac{\pi}{6}a^4}}{\rho}. \quad (5.33)$$

We then incorporate the first term from Eq. 5.25:

$$\frac{4}{\sqrt{6}}\sqrt{\rho}\left(1 - \rho\frac{1 - e^{-\rho\frac{\pi}{6}a^4}}{\rho}\right) = -\frac{4}{\sqrt{6}}\sqrt{\rho}e^{-\rho\frac{\pi}{6}a^4}, \quad (5.34)$$

which, using the argument from R_3, clearly goes to zero in the limit.

Now we must show that R_2 goes to zero as well:

$$R_2(p) = 4\pi \int_a^{T_p\sqrt{2}} dv \int_0^{\frac{a^2}{v}} du \, \frac{1}{2}(v-u)^2 \left(1 - 9\rho V + 8(\rho V)^2 - \frac{4}{3}(\rho V)^3\right) e^{-\rho V}, \quad (5.35)$$

with $V = \frac{\pi}{6}u^2v^2$ and having performed the polar integrals. Mathematica performs both integrals:

$$\begin{aligned} R_2(p) =& \frac{\pi}{27}a^2 e^{-\rho\frac{\pi}{6}a^4} \\ & \left(-\frac{9a^4}{2T_p^2} - 54a^2\log(T_p) - 18a^2 - 27a^2\log(2) + 54a^2\log(a) + 54T_p^2\right. \\ & + \rho\left(\frac{15\pi a^8}{4T_p^2} + 36\pi a^6\log(T_p) + 3\pi a^6 + 18\pi a^6\log(2) - 36\pi a^6\log(a)\right. \\ & \left.-21\pi a^4 T_p^2\right) \\ & + \rho^2\left(-\frac{\pi^2 a^{12}}{4T_p^2} - 2\pi^2 a^{10}\log(T_p) - \pi^2 a^{10}\log(2) + 2\pi^2 a^{10}\log(a)\right. \\ & \left.\left.+\pi^2 a^8 T_p^2\right)\right). \end{aligned} \quad (5.36)$$

This integral is exponentially suppressed by the exponential factor, which then follows the same arguments made previously for R_3 and R_2. However, we should notice that an assumption has been made, but not justified. To see this consider the green circled region in Fig. 5.5, shown more clearly in Fig. 5.6. While [3] does verify that the contribution from W_2 goes to zero, it does not take into account the possibility of a hard cutoff, for instance, the top of the slab. Applying this allows us to identify three regions: A_1, A_2 and the remaining $(W_2 - A_1 - A_2)$. We must then show that either contribution D_1 or D_2, from A_1 or A_2, goes to zero.

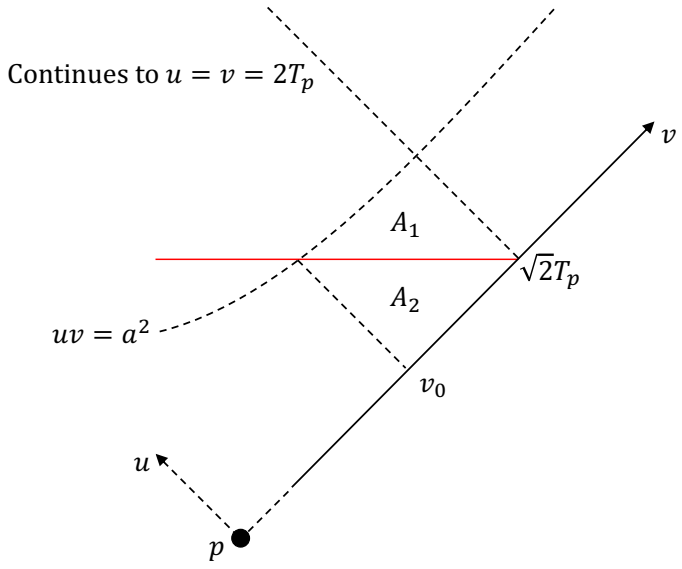

Figure 5.6: A clearer picture of the green circle in Fig. 5.5, A_1 and A_2 are part of W_2. The top of the slab, i.e. the end of support for field φ is represented by the red line.

For completeness, the bounds of null integration for both regions are:

$$A_1: \qquad u \in \left[\sqrt{2}T_p - v, \frac{a^2}{v}\right] , \qquad v \in \left[v_0, \sqrt{2}T_p\right] , \tag{5.37}$$

$$A_2: \qquad u \in \left[0, \sqrt{2}T_p - v\right] , \qquad v \in \left[v_0, \sqrt{2}T_p\right] , \tag{5.38}$$

and we have that $v_0 = \frac{T_p}{\sqrt{2}} + \sqrt{\frac{T_p^2}{2} - a^2}$. We choose to integrate over A_2 as it is most

similar to our original problem:

$$D_2(p) = 4\pi \int_{v_0}^{\sqrt{2}T_p} dv \int_0^{\sqrt{2}T_p - v} du \, \frac{1}{2}(v-u)^2 \left(1 - 9\rho V + 8(\rho V)^2 - \frac{4}{3}(\rho V)^3\right) e^{-\rho V} . \tag{5.39}$$

Mathematica is able only to perform the u integral analytically, which is precisely the result in Eq. 5.22 (up to the bounds of the v integral). Now to tackle the v integral, we will use numerical methods on Mathematica. To do this, we must set our variables, and we choose:

$$T_p = \frac{1}{\sqrt{2}}, \qquad a = \rho^{-\frac{1}{8}}, \tag{5.40}$$

and we also take in the extra $\rho^{3/2}$ factor from Eq. 5.25. Finally we may numerically integrate for $\rho \in [10^4, 10^8]$. We may then fit a function to our output, $g(\rho) \sim -\rho^{-1/2}$, which behaves as we expect, Fig. 5.7. This clearly goes to zero in the limit, and so the assumption made in [3] holds.

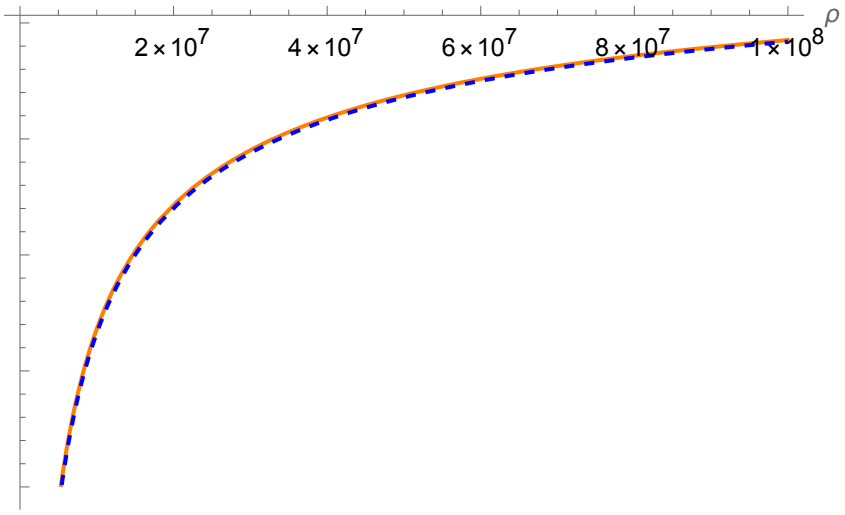

Figure 5.7: A plot showing the numerical integration of $-\rho^{3/2} D_2$ — plotted with the fitted function $g(\rho)$ - - -, for varying ρ on the x-axis and fixed $T_p = \frac{1}{\sqrt{2}}$, $a = \rho^{-1/8}$. A clear agreement may be seen, and both approach zero as $\rho \to \infty$.

The v Integral: Part Two

We now return to $I_{\mathrm{I}}(p)$ and $I_{\mathrm{II}}(p)$, and place them back into our expression for $L_\rho(p)$:

$$L_\rho(p) = \frac{4}{\sqrt{6}}\sqrt{\rho}\left[1 - \rho\left(I_{\mathrm{I}}(p) + I_{\mathrm{II}}(p)\right)\right] . \tag{5.41}$$

We split this expression in two:

$$L_\rho(p) = K_{\mathrm{I}}(p) + K_{\mathrm{II}}(p) , \tag{5.42}$$

where:

$$\begin{aligned} K_{\mathrm{I}}(p) &= \frac{4}{\sqrt{6}}\sqrt{\rho}\left(1 - \rho I_{\mathrm{I}}(p)\right) \\ &= \frac{4}{\sqrt{6}}\sqrt{\rho}e^{-\rho\frac{\pi}{24}T_p^4} , \end{aligned} \tag{5.43}$$

$$K_{\mathrm{II}}(p) = -\frac{4}{\sqrt{6}}\rho^{\frac{3}{2}}I_{\mathrm{II}}(p) . \tag{5.44}$$

we note that while K_{I} has been calculated analytically and clearly $\to 0$ as $\rho \to 0$, the second still cannot be computed, and we do not yet know its behaviour. Using the results from Belenchia et al. [3], we may notice that K_{II} is the same as R_2 up to the lower bound of the v integral. However, as the lower bound in R_2 is ρ-dependent through a, we will explicitly verify the behaviour of K_{II} in the limit.

Again, for numerical integration, we must assign values to the variables we are not investigating:

$$T_p = \frac{1}{\sqrt{2}} , \tag{5.45}$$

and numerically integrate for $\rho \in [10^4, 10^8]$. The fitted function, $g'(\rho) \sim -\rho^{-1/2}$, does not agree as well as it does for that of R_2 in Fig. 5.7. Nevertheless, it behaves as expected and approaches zero in the limit, see Fig. 5.8. This disagreement may be explained by higher order terms having a stronger influence on K_{II}.

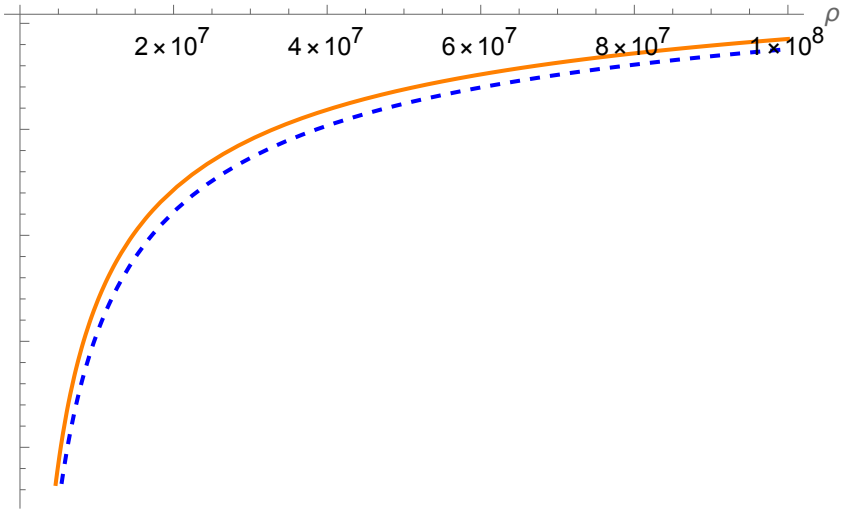

Figure 5.8: A plot showing the numerical integration of $K_{\mathrm{II}}(p)$ — plotted with the fitted function $g'(\rho)$ - - -, for varying ρ on the x-axis and fixed $T_p = \frac{1}{\sqrt{2}}$. A satisfactory agreement may be seen, and both approach zero as $\rho \to \infty$.

5.4 The Outer Integral

Moving onto the outer integral, the one in Eq. 4.7, we may put all we have together:

$$\frac{1}{\hbar}\langle \boldsymbol{\mathcal{S}}_\rho(\mathcal{M})\rangle = \frac{1}{l_p^{d-2}}\int_{\mathcal{M}} d^d p\,(K_{\mathrm{I}} + K_{\mathrm{II}})\ . \tag{5.46}$$

This integral is performed over the full manifold, shown in Fig. 5.1; we may simply use the original $\{x^\mu\}$ coordinates, similarly to what we did for the Einstein-Hilbert term, see Sec. 5.2. The bounds of integration for this integral will simply be:

$$x^0 \in [0, T]\ , \qquad x^i \in [0, L]\ , \tag{5.47}$$

and noticing that the integrand is independent of x^i due to the spatial translation invariance, it is straightforward to see that the d^3x^i integral evaluates to an L^3 factor. We will assume this integral has been done, note that $x^0 \equiv p^0$, and recall that $T_p = T - p^0$. We now split Eq. 5.46 into two terms, as they are evaluated differently:

$$H_{\mathrm{I}} = L^3 \frac{4}{\sqrt{6}}\sqrt{\rho}\int_0^T dp^0\, e^{-\rho\frac{\pi}{24}\left(T-p^0\right)^4}\ , \tag{5.48}$$

and:

$$H_{\mathrm{II}} = L^3 \int_0^T dp^0 \, K_{\mathrm{II}}\,(p) \ . \tag{5.49}$$

Before evaluating the p^0 integrals and verifying the behaviour of these expressions in the continuum limit, we should investigate how the integrands of H_{I}, H_{II} behave over $p^0 \in [0,\, T]$, to make sure there is no "funny business" near the top boundary. Clearly, the integrand of H_{I} is well-behaved over the domain of p^0, however, we should look into that of H_{II}. We may plot it for:

$$T = 1\,, \qquad \rho = 10^7\,, \tag{5.50}$$

in Fig. 5.9.

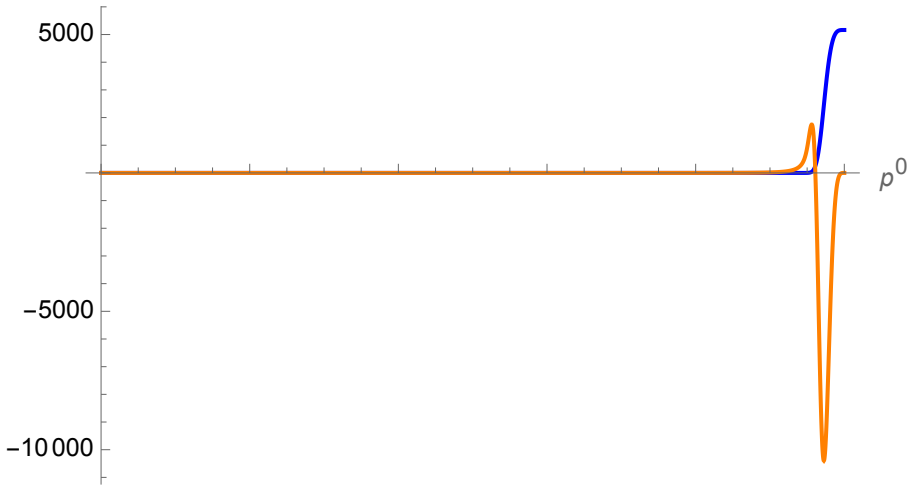

Figure 5.9: A plot showing the integrands of H_{I} — and H_{II} —, for $p^0 \in [0, T]$ with $T = 1$, $\rho = 10^7$. Both functions have finite areas and are well-behaved over the domain of p^0.

Both integrands are well-behaved over the domain, so we may now move on and check the behaviour in the limit. We also note that with increasing ρ, the two functions tend towards narrower and more elongated peaks, with H_{II}'s moving towards $p^0 = T$.

Returning to the integrals, we are able to evaluate H_{I} analytically using Mathe-

matica:

$$H_{\mathrm{I}} = \left(\frac{2}{3\pi}\right)^{\frac{1}{4}} \rho^{\frac{1}{4}}\, \Gamma\left(\frac{1}{4}\right) - \frac{1}{\sqrt{6}}\sqrt{\rho}\, \mathrm{ExpIntegralE}\left[\frac{3}{2},\, \frac{\pi}{24}\rho\right] , \tag{5.51}$$

while H_{II} has to be done numerically. Performing this double numerical integration is trickier as we have implicit bounds, specifically:

$$H_{\mathrm{II}}\text{:} \qquad v \in \left[\frac{T-p^0}{\sqrt{2}}, \sqrt{2}\left(T-p^0\right)\right] , \qquad p^0 \in [0, T] \ . \tag{5.52}$$

To resolve this issue, we may plot our bounds of integration on a $(p^0 - v)$ plane and notice that they form a triangle with coordinates:

$$\left(p^0,\, v\right) : \qquad (T\,, 0)\ , \qquad \left(0\,, \frac{T}{\sqrt{2}}\right) , \qquad \left(0\,, \sqrt{2}T\right) . \tag{5.53}$$

Fortunately, Mathematica is able to perform a numerical integral over an area, and it gives finite values.

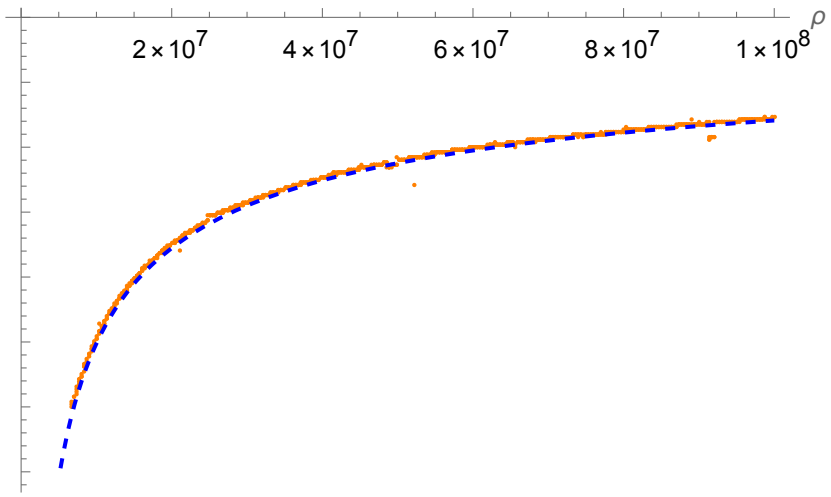

Figure 5.10: A plot showing the discrete numerical integration of $H_{\mathrm{I}}(p) + H_{\mathrm{II}}(p)$ •, plotted with the fitted function $g''(\rho)$ - - -, for varying ρ on the x-axis and fixed $T = 1$. A satisfactory agreement may be seen, and both approach zero as $\rho \to \infty$.

To analyse the behaviour in the limit, we numerically evaluate $H_{\mathrm{I}} + H_{\mathrm{II}}$ for increasing values of ρ and set $T = 1$, see Fig 5.10. We note that we had to perform the integration in discrete steps of $\Delta\rho = 10^5$ for $\rho \in [10^4, 10^8]$, some discrepancy in

the form of anomalous points is down to "precision error" as stated by Mathematica output warnings. The fitted function, $g''(\rho) \sim -\rho^{-1/2}$, goes with the mean scalar action, $\langle \boldsymbol{\mathcal{S}}_\rho(\mathcal{M}) \rangle = H_{\mathrm{I}} + H_{\mathrm{II}}$.

We can then see that:

$$\lim_{\rho \to \infty} \langle \boldsymbol{\mathcal{S}}_\rho(\mathcal{M}) \rangle = 0\,, \tag{5.54}$$

as was conjectured by Benincasa and Dowker, Sec. 5.2 [46].

Chapter 6

Discussion

Causal set theory is a programme for quantum gravity. It postulates that, fundamentally, spacetime is a discrete collection of events that grow in time and whose structure is sourced purely from its causal order. It postulates that there is a continuum limit when the density of elements is so large that discreteness of spacetime is no longer apparent, recovering the well-known and established quantum field theory and theory of general relativity. In formulating this, a quantum causal dynamics is required to build a full theory of quantum gravity; this based on a sum-over-histories framework for which a well-formulated action is required. The behaviour of the Benincasa-Dowker-Glaser action and its building block, the discretised d'Alembertian operator, in the limit was the focus of this project.

A previously unjustified but assumed condition that arises when looking at how the discretised d'Alembertian acts on a causal set faithfully embedded in Minkowski spacetime was successfully verified. The original paper broke down a manifold into three regions, two of which were independent of the support of the scalar field φ and thus would always be "exponentially suppressed". The remaining region's boundaries of integration are however dependent on the boundary of support of φ. Belenchia et al. performed this calculation but missed to consider the case for where the support acted as it does in this work: a hard horizontal cutoff. This specific cutoff

results in two new regions, either of which must have a contribution equal to zero in order for the assumption to hold. Unlike for the other regions, the result is not immediately obvious as there is no exponential suppression, and analytical results are not immediately available using Mathematica. Therefore, numerical methods were utilised. The result was explicitly verified, successfully showing that the assumption stands and thus reinforcing the paper by Belenchia et al..

With the use of this result, the Benincasa-Dowker conjecture was confirmed for the case of a four-dimensional slab with spatial antipodal identification embedded in flat Minkowski spacetime. The conjectured result for this spacetime is purely the Einstein-Hilbert action (which is equal to zero in flat spacetime) without any extra joint boundary term due to the lack of intersection between the future- and past-boundaries of the slab. Due to Mathematica being unable to perform integrals of a certain form, a combination of numerical and analytical methods were employed to reach a solution. Furthermore, in order to be able to numerically integrate the functions, the behaviour of the integrands was verified over the full range of integration. Finally, the mean discrete causet action (BDG) was shown to approach zero in the continuum limit $\rho \to \infty$ as $\sim -\rho^{-1/2}$, in agreement with the Benincasa-Dowker conjecture

Nevertheless, there is much more work to be done regarding the conjecture, not only the extension of this example to curved spacetime but also perhaps a formal proof for it as a whole. From the studied case, and from those examples present in the literature [46, 47, 50, 51, 52, 53], it is anything but easy to see how and why the boundary terms appear as a result of the joint. Determining how to spot this, possibly by writing the mean discrete action in a different form, would greatly simplify the gathering of evidence and move us down the path of proving the conjecture with greater generality. An extension to arbitrary curvature using Riemann normal coordinates for specific geometries is present in the literature. Further extending this to generic geometries would greatly benefit the move towards

a full proof.

Should the conjecture hold, it would be a strong move towards building up the sum-over-histories approach. As explained by Dowker [47], such a result would suggest that the originally non-local BDG action can indeed be localised by the continuum limit and be well-behaved in the presence of curvature. This contrasts with the non-manifold-like family of causal sets, which have a non-local action. Thus, it would give a clear distinguishing property that could be used when picking out the manifold-like causal sets in the sum-over-histories framework.

Amending the lack of knowledge on the discretised scalar d'Alembertian in generic curvature could reinforce the arguments for the conjecture regarding the Einstein-Hilbert term. As Dowker suggests [47], in the short term, computational and numerical methods involving the modified d'Alembertian (with dampened fluctuations) could achieve this result while analytical approaches continue to be studied. However, analysing the asymptotic regime remains no easy task due to the sheer number of elements in the causet. Also, the reasoning behind the construction of the d'Alembertian, and the origin of, or reasons for why, the curious sequence of minimum layers required for coefficient uniqueness is the way it is could be an exciting area of study. They may bring to light some novel ideas.

Furthermore, advances are to be made in the study of the action itself. The BDG action, although widely successful, is dimensional-dependent. Imposing a dimension does not seem like a reasonably fundamental act. We should be asking ourselves *why* our reality appears to be in four dimensions, not imposing it arbitrarily in our many models. We would like for $d = 4$ to appear out of these models. Therefore, a more fundamental version of the action could still be out there, hidden from view, perhaps in a quantum sequential growth model. The discovery of such an action could also provide insight regarding the previous comments on the d'Alembertian uniqueness. Notwithstanding, this would not necessarily disprove the BDG action; it may govern an intermediate regime of the theory, so it, and its many uses and

applications, should continue to be investigated.

Further work could also be done in exploring the behaviour of the BDG action and discretised scalar d'Alembertian for more general geometries (for instance, those which include timelike boundaries). Although this conjecture is only made with globally hyperbolic spacetimes in mind, a more general analytical extension could exist. Additionally, investigating the behaviour of the discretised scalar d'Alembertian on a varying scalar field for a general spacetime geometry with arbitrary curvature could lead to compelling results.

Regardless of this conjecture's outcome, I have but one wish. I wish for the result to give way to novel ideas, shine a light on our still-obscure universe, and lead to a deeper understanding of this beautifully elegant theory of geometry from causality and discreteness.

"Success is not final, failure is not fatal: it is the courage to continue that counts."

Sir Winston Churchill

Bibliography

[1] C. J. Fewster, E. Hawkins, C. Minz, and K. Rejzner, "Local structure of sprinkled causal sets," *Physical Review D*, vol. 103, no. 8, p. 086020, 2021.

[2] J. Henson, "The causal set approach to quantum gravity," *Approaches to quantum gravity: towards a new understanding of space, time and matter*, vol. 393, 2009.

[3] A. Belenchia, D. M. Benincasa, and F. Dowker, "The continuum limit of a 4-dimensional causal set scalar d'alembertian," *Classical and Quantum Gravity*, vol. 33, no. 24, p. 245018, 2016.

[4] C. Rovelli, "Loop quantum gravity," *Living reviews in relativity*, vol. 11, no. 1, pp. 1–69, 2008.

[5] K. R. Dienes, "String theory and the path to unification: A review of recent developments," *Physics Reports*, vol. 287, no. 6, pp. 447–525, 1997.

[6] R. D. Sorkin, "Spacetime and causal sets.," *Relativity and Gravitation*, p. 150, 1991.

[7] M. E. Peskin, *An introduction to quantum field theory*. CRC press, 2018.

[8] A. Shomer, "A pedagogical explanation for the non-renormalizability of gravity," *arXiv preprint arXiv:0709.3555*, 2007.

[9] S. W. Hawking and R. Laflamme, "Baby universes and the non-renormalizability of gravity," *Physics Letters B*, vol. 209, no. 1, pp. 39–41, 1988.

[10] G. Hooft, "Quantum gravity: a fundamental problem and some radical ideas," in *Recent Developments in Gravitation*, pp. 323–345, Springer, 1979.

[11] K. S. Thorne, C. W. Misner, and J. A. Wheeler, *Gravitation*. Freeman San Francisco, CA, 2000.

[12] B. P. Abbott, R. Abbott, T. Abbott, M. Abernathy, F. Acernese, K. Ackley, C. Adams, T. Adams, P. Addesso, R. Adhikari, *et al.*, "Observation of gravitational waves from a binary black hole merger," *Physical review letters*, vol. 116, no. 6, p. 061102, 2016.

[13] E. H. T. Collaboration, K. Akiyama, A. Alberdi, W. Alef, K. Asada, R. AZULY, *et al.*, "First m87 event horizon telescope results. i. the shadow of the supermassive black hole," *Astrophys. J. Lett*, vol. 875, no. 1, p. L1, 2019.

[14] Q. Bonnefoy, L. Ciambelli, D. Lüst, and S. Lüst, "Infinite black hole entropies at infinite distances and tower of states," *Nuclear Physics B*, vol. 958, p. 115112, 2020.

[15] S. W. Hawking, "Gravitational radiation from colliding black holes," *Physical Review Letters*, vol. 26, no. 21, p. 1344, 1971.

[16] R. D. Sorkin, "Forks in the road, on the way to quantum gravity," *International Journal of Theoretical Physics*, vol. 36, no. 12, pp. 2759–2781, 1997.

[17] B. Riemann and H. Weyl, "Über die hypothesen, welche der geometrie zugrunde liegen," in *Über die Hypothesen, welche der Geometrie zu Grunde liegen*, pp. 1–47, Springer, 1919.

[18] A. Einstein, "Letter to hs joachim, august 14, 1954, item 13-453, cited in j. stachel,"einstein and the quantum: Fifty years of struggle" in from quarks, philosophical problems of modern physics (rg colodny, ed.) u," 1986.

[19] R. D. Sorkin, "Causal sets: Discrete gravity," in *Lectures on quantum gravity*, pp. 305–327, Springer, 2005.

[20] S. W. Hawking, A. R. King, and P. McCarthy, "A new topology for curved space–time which incorporates the causal, differential, and conformal structures," *Journal of mathematical physics*, vol. 17, no. 2, pp. 174–181, 1976.

[21] D. B. Malament, "The class of continuous timelike curves determines the topology of spacetime," *Journal of mathematical physics*, vol. 18, no. 7, pp. 1399–1404, 1977.

[22] S. Surya, "The causal set approach to quantum gravity," *Living Reviews in Relativity*, vol. 22, no. 1, pp. 1–75, 2019.

[23] A. Levichev, "Prescribing the conformal geometry of a lorentz manifold by means of its causal structure," in *Soviet Math. Dokl*, vol. 35, p. 133, 1987.

[24] R. D. Sorkin, "First steps with causal sets," tech. rep., Syracuse Univ., Syracuse, NY, 1991.

[25] J. F. C. Kingman, *Poisson processes*, vol. 3. Clarendon Press, 1992.

[26] L. Bombelli, J. Henson, and R. D. Sorkin, "Discreteness without symmetry breaking: a theorem," *Modern Physics Letters A*, vol. 24, no. 32, pp. 2579–2587, 2009.

[27] J. Myrheim, "Statistical geometry," tech. rep., CERN, 1978.

[28] D. A. Meyer, "Spherical containment and the minkowski dimension of partial orders," *Order*, vol. 10, no. 3, pp. 227–237, 1993.

[29] D. A. Meyer, *The dimension of causal sets*. PhD thesis, Massachusetts Institute of Technology, 1988.

[30] D. D. Reid, "Manifold dimension of a causal set: Tests in conformally flat spacetimes," *Physical Review D*, vol. 67, no. 2, p. 024034, 2003.

[31] D. P. Rideout and R. D. Sorkin, "Classical sequential growth dynamics for causal sets," *Physical Review D*, vol. 61, no. 2, p. 024002, 1999.

[32] D. Rideout, "Dynamics of causal sets," *Physics - Dissertations and Theses*, 01 2003.

[33] R. D. Sorkin, "Quantum mechanics as quantum measure theory," *Modern Physics Letters A*, vol. 9, no. 33, pp. 3119–3127, 1994.

[34] R. D. Sorkin, "Quantum measure theory and its interpretation," *arXiv preprint gr-qc/9507057*, 1995.

[35] S. Surya and S. Zalel, "A criterion for covariance in complex sequential growth models," *Classical and Quantum Gravity*, vol. 37, no. 19, p. 195030, 2020.

[36] S. Surya, "Evidence for the continuum in 2d causal set quantum gravity," *Classical and Quantum Gravity*, vol. 29, no. 13, p. 132001, 2012.

[37] L. Bombelli, J. Lee, D. Meyer, and R. D. Sorkin, "Space-time as a causal set," *Physical review letters*, vol. 59, no. 5, p. 521, 1987.

[38] C. Moore, "Comment on "space-time as a causal set"," *Physical Review Letters*, vol. 60, no. 7, p. 655, 1988.

[39] L. Bombelli, J. Lee, D. Meyer, and R. D. Sorkin, "Bombelli et al. reply," *Physical Review Letters*, vol. 60, no. 7, p. 656, 1988.

[40] D. M. Benincasa and F. Dowker, "Scalar curvature of a causal set," *Physical review letters*, vol. 104, no. 18, p. 181301, 2010.

[41] R. D. Sorkin, "Does locality fail at intermediate length-scales," *Approaches to quantum gravity: Toward a new understanding of space, time and matter*, pp. 26–43, 2009.

[42] S. Aslanbeigi, M. Saravani, and R. D. Sorkin, "Generalized causal set d'alembertians," *Journal of High Energy Physics*, vol. 2014, no. 6, pp. 1–25, 2014.

[43] F. Dowker and L. Glaser, "Causal set d'alembertians for various dimensions," *Classical and Quantum Gravity*, vol. 30, no. 19, p. 195016, 2013.

[44] L. Glaser, "A closed form expression for the causal set d'alembertian," *Classical and Quantum Gravity*, vol. 31, no. 9, p. 095007, 2014.

[45] D. Oriti, *Approaches to quantum gravity: Toward a new understanding of space, time and matter*. Cambridge University Press, 2009.

[46] D. M. T. Benincasa, *The action of a casual set*. PhD thesis, Imperial College London, 2013.

[47] F. Dowker, "Boundary contributions in the causal set action," *Classical and Quantum Gravity*, vol. 38, no. 7, p. 075018, 2021.

[48] H. Reall, "Part 3 black holes," *Lecture notes given as part of the Cambridge University Mathematical Tripos*, 2014.

[49] G. Gibbons and S. Solodukhin, "The geometry of small causal diamonds," *Physics Letters B*, vol. 649, no. 4, pp. 317–324, 2007.

[50] D. M. Benincasa, F. Dowker, and B. Schmitzer, "The random discrete action for two-dimensional spacetime," *Classical and Quantum Gravity*, vol. 28, no. 10, p. 105018, 2011.

[51] A. Bhatnagar, "Causal set theory and the benincasa-dowker conjecture," Master's thesis, Imperial College London, 2021.

[52] M. Buck, F. Dowker, I. Jubb, and S. Surya, "Boundary terms for causal sets," *Classical and Quantum Gravity*, vol. 32, no. 20, p. 205004, 2015.

[53] L. Machet and J. Wang, "On the continuum limit of benincasa–dowker–glaser causal set action," *Classical and Quantum Gravity*, vol. 38, no. 1, p. 015010, 2020.